Pluriannual beach-dune evolutions at regional scale: Erosion and recovery sequences analysis along the aquitaine coast based on airborne LiDAR data

Alexandre Nicolae Lerma, Bruce Ayache, Beatrice Ulvoas, François Paris, Nicolas Bernon, Thomas Bulteau, Cyril Mallet

Pluriannual beach-dune evolutions at regional scale: Erosion and recovery sequences analysis along the Aquitaine coast based on airborne LiDAR data

Authors: Alexandre Nicolae Lerma, Bruce Ayache, Beatrice Ulvoas, François Paris, Nicolas Bernon, Thomas Bulteau, Cyril Mallet

Corresponding author: a.nicolaelerma@brgm.fr

Affiliation: BRGM (French Geological Survey), Direction Régionale Nouvelle-Aquitaine, Parc Technologique Europarc, 24 avenue Léonard de Vinci, 33600 Pessac, France,

Abstract:

With apparent uniformity, the 230 kilometers of the Aquitanian sandy coast presents many differences in geomorphological characteristics and evolutions at the event, seasonal, annual and pluriannual time scales. This contribution highlights work based on extensive airborne LiDAR coverage campaigns realized in 2011, 2014, 2016 and 2017. Geomorphological evolutions are studied at the scale of the sedimentary cell and subcells of the Aquitanian sandy coast, specifically through the automatic detection of dune erosion scarps and incipient foredunes, the planimetric indicators of foredunes, dune feet and dune front evolutions along the coast, and the sediment budget of the beach-dune interface. Analyses were performed for two periods: 2011-2014 (including the erosional impact of the 2013-2014 winter) and 2014-2017, presenting continuous and extensive beach recovery at the beach-dune interface. Dune erosion scarps and incipient foredune characteristics are analyzed in term of alongshore length, width, surface and shape. A classification based on the alongshore length of the erosion scarp shows great diversity of erosional dynamics, which are directly linked to the geomorphologic characteristics of the beach sediment availability and the nearshore bar system. This diversity includes homogeneously large erosional bands above a 1 km alongshore length, periodic Mega cusp embayments from 200 to 800 m, and a local erosion mark less than 200 m long. Analysis for the following period shows a prompt and massive recovery at the upper beach and dune foot proxies on the majority of the coast. However, the recovery process as well as erosion is strongly marked by a North–South gradient. The dune front was massively impacted in Gironde, with a retreat exceeding 25 m that was poorly prograded since 2014, whereas in Landes a progradation of the front dune is observed compared to 2011. During the first period (including the 2013-2014 winter), more than 15 500 × 10^3 m^3 of sediment was eroded from the beach-dune interface, which represents on average a loss of 66 m^3 per linear meter. The gains during the following period (2014-2017) are also massive, above 13 500 × 10^3 m^3, with an average gain of 57 m^3 per linear meter. Given the budget between the two periods, 86.5 % of the sand eroded in 2014 had moved back in 2017 at the beach-dune interface but was generally further south following the dominant north-south alongshore drift. At the pluriannaual, decadal and pluridecadal scales, the different sections of the coast follow various trends concerning erosion as well as recovery processes.

Key words: Airborne LiDAR, beach-dune interface, massive erosion, erosion scarp, pluriannual recovery, incipient foredune, sediment budget

Introduction

Beach-dune systems as an interface between the marine and terrestrial environments constitute a buffer zone against marine hazards. Dune retreat is generally the consequence of major storm events and characterizes the erosion hazard. Dunes are also considered as the first line of defense against flooding. Over many years, evolutions of the dune front during storm conditions were observed and analyzed in many places around the world (e.g., Vellinga, 1982, Pye and Neal, 1994; Sallenger, 2000; Esteves et al., 2012; Almeida et al., 2012; Houser, 2013; Splinter et al., 2014; Palmsten et al., 2014; Dissanayake et al., 2015; Castelle et al.,2015). More recently, observations and analyses of the factors of post storm dune recovery have been a subject of increasing attention (Matias et al., 2004; Houser and Hamilton 2009; Vousdoukas et al., 2012; Scott et al., 2016; Castelle et al., 2017). Recovery processes have been analyzed at various time scales from days (Wang et al., 2006; Coco et al., 2014; Aungnuureng et al., 2017; Segura et al., 2018) to months (Senechal et al., 2015; Phillips et al., 2017), years (Castelle et al., 2017, Burvingt et al., 2017), or decades (Houser et al., 2015).

Several techniques can be used to study beach-dune interfaces, but these techniques vary in terms of their applicability at different spatial and temporal scales. For example, d-GPS campaigns are still regularly used for event surveys (pre and post storm survey, Biausque and Senechal 2018; Castelle et al., 2017, Brenner et al., 2018) but are limited to small coastal sections (hundreds meters to few kilometers). UAV photogrammetric campaigns are increasingly used to survey dunes and beaches (Gonçalves and Henriques, 2015; Turner et al., 2016). They provide useful information for studying seasonal evolutions and provide very high-resolution data, but they are nevertheless limited to a few kilometers in coverage; additionally, post-treatment processing is still complex, presenting variable vertical accuracy results.

In the past 20 years, LiDAR surveys have been routinely used to study coastal evolutions, quantitative beach morphology changes (Sallenger et al., 2003), dune morphodynamics and volumetric changes (Andrews et al., 2002; Woolard and Colby, 2002) and even subtidal morphology with adapted sensors in clear coastal waters (Irish and White, 1998; Pastol, 2011; Aleman et al., 2015). Many studies have investigated coastal dunes using LiDAR. They focused on morphologic features or volumetric information over time (among many others, Woolard and Colby, 2002; Richter et al., 2013; Keijsers et al., 2014, 2015), storm morphological impacts (Saye et al., 2005; Houser et al., 2008, 2015, Pye and Blott 2016, Burvingt et al., 2017) or foredune biogeomorphic interactions (Keijsers et al., 2015; Doyle and Woodroffe, 2018).

Airborne LiDAR offers a useful solution for obtaining topographic information of coastal dunes and intertidal areas, providing post treatment, gridded 1–2 m spatial resolution DTMs, typically with a 15–20 cm vertical accuracy and potentially covering several hundred kilometers. They offer extensive data sets to analyze large-scale coastal evolutions (Scott et al., 2016, Burvingt et al., 2017). Even if LiDAR campaigns are relatively expensive and are time consuming due to post treatments, annual repetition of this kind of survey at post winter or post summer periods provide very valuable data to study the spatial variability of storm impacts or recovery sequences along large continuous coastlines (Houser et al., 2015). LiDAR's large coverage area and relatively accurate 3D data also offer high potential for morphometric parameter definitions (Woolard and Colby, 2002; Saye et al., 2005; Brock and Purkis 2009; Burvingt et al. 2018, LeMauff et al., 2018).

Poorly urbanized (less than 10 %) and presenting an almost continuous 230 km long open beach-dune system, the sandy Aquitaine Coast is globally affected by erosion. Since 1985, Bernon et al., 2016 the coastline has retreated at 2.5 m/year on average in Gironde and at 1.7 m/year on average in Landes. However, along the Aquitaine coast, the erosion rate at the pluri-decadal scale (Castelle et al., 2018) and at the seasonal scale (Bulteau et al., 2014) can have high geographic variability.

The aim of this study is first to characterize the impact of the extremely active 2013-2014 winter at regional scale, as it represented the highest winter-mean wave energy level since at least 1948 (Masselink et al., 2016). Second, the progressive recovery between 2014 and 2017 along the Aquitaine coast is analyzed. Erosion and recovery phases are characterized through automatic detection of the erosional dune scarp and incipient foredune. Beach-dune evolutions are also investigated through several cross-shore morphometric indicators and volumetric changes. Then, the 2011-2017 evolutions are analyzed for the coastline evolution and volumetric budget. The results are finally discussed, and a conceptual model of the recovery stages is proposed before drawing the conclusions.

2. Materials and Methods

2.1 Site

The sandy Aquitaine coast extends from the Gironde Estuary at the north to the Adour River at the south (Figure 1). It is an almost continuous 230 km long open beach-dune system (mainly interrupted by the inlet of the Arcachon lagoon). The continuous coastline of Gironde and Landes shows significantly different alongshore characteristics and was divided into relatively homogeneous sedimentary cells or subcells (Le Nindre et al., 2001; BRGM and ONF, 2017) based on several morphological and dynamic criteria; these criteria include the dominant longshore drift (Idier et al., 2013), nearshore sandbars configuration (Castelle et al., 2007), beach slope (Bulteau et al., 2016), sediment grain size (Pedreros, 2000), seaward shelf width, beach width and the coastal dune system (BRGM and ONF, 2017) (Figure 1). Table 1 synthetizes the main geomorphological characteristics of the nearshore and beach-dune interface along the coast, while a full description of the segmentation of the coast is detailed in BRGM and ONF (2017).

The coast is quite homogenously exposed to the Atlantic swell both annually (Castelle et al., 2017) and during extreme storm conditions (Nicolae Lerma et al., 2015). The annual offshore wave means are approximately 1.8 m and 11.5 s for significant wave height *(Hs*) and peak period (*Tp),* respectively. Extreme offshore *Hs* conditions defined here as 100-year return values are also quite similar, with a slight increase from north (*Hs* = 11 m) to south (*Hs* = 11.6 m) (Nicolae Lerma et al., 2015).

The mean wave directions are from the west in the northern part of the coast, whereas the directions are from the northwest in the south of the coast, explaining relatively to the orientation of the coast the general characteristics of the longshore drift (Idier et al., 2013) (Figures 1 and 2). Along the coast, the longshore drift is generally southward oriented except for Cell 1, and Cells 6.1 and 6.2 showed that the annual residual dominant direction is northward-oriented. Annual residual flux volumes estimated by Idier et al., 2013 are on average between 200 000 to 400 00 m^3/y in Gironde, with a local substantial increase at the Cap Ferret spit with 657 000 m^3/y. The residual flux in Landes decrease from Cell 4 to Cell 5.3 from 700 000 to 500 000 m^3/y. At Cells 6.1 and 6.2, due to a change in the orientation of the coast and coarser sediment, the flux is reduced and the directions are more contrasted, as the residual flux is at 40 000 m^3/y northward-oriented.

Wind orientation at the Aquitaine Coast is quite homogenous along the coast except at the extreme south, where offshore winds are overrepresented in comparison with the rest of the coast (Figure 2). Winter winds mainly come from the west whereas dominant spring and summer winds (from April to September) come from the northwest and north. Main constructive winds, which are prone to accumulating sand at the dune foot, mostly come from the north or south with velocity > 5 m/s respectively to the typical median grain size (0.03 mm). Relative to the main orientation of the coast, these directions allow longer fetches and thus a larger transport capacity. Westerly winds can also contribute to foredune growth, but only where the beach systems are the widest in the southern Gironde (Cells 3.5, 4) and Landes coasts (Cell 5.1 to 5.3). Previous studies have reported significant contribution of aeolian flux of sand to sediment mobility along the coast. In Gironde Froidefond and Prud'homme

(1991) estimated the flux at 15 to 30 m3/m/yr before the fixation of the dune but Aubié and Tastet 2000 considered that aeolian sand loss moving landward is today almost negligible.

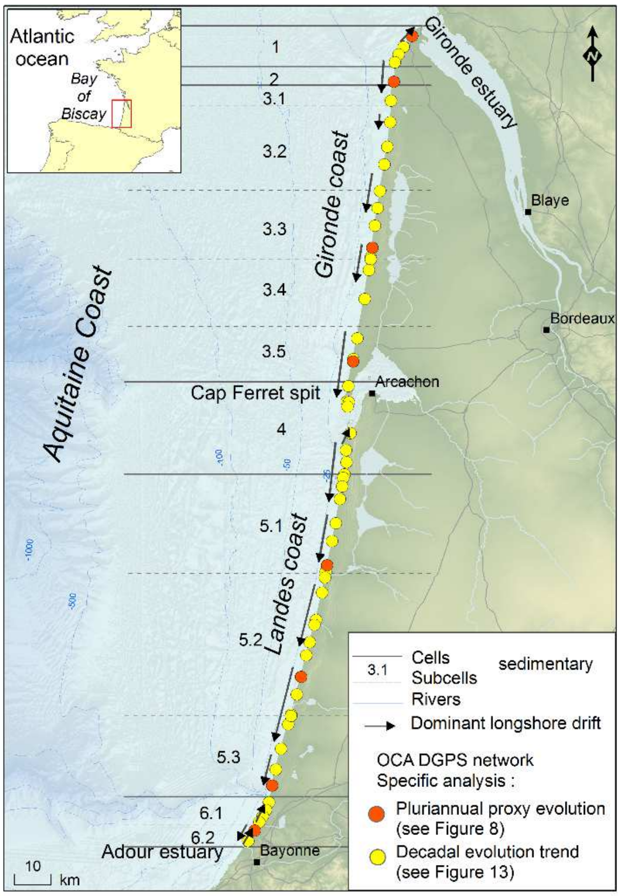

Figure 1: Location map

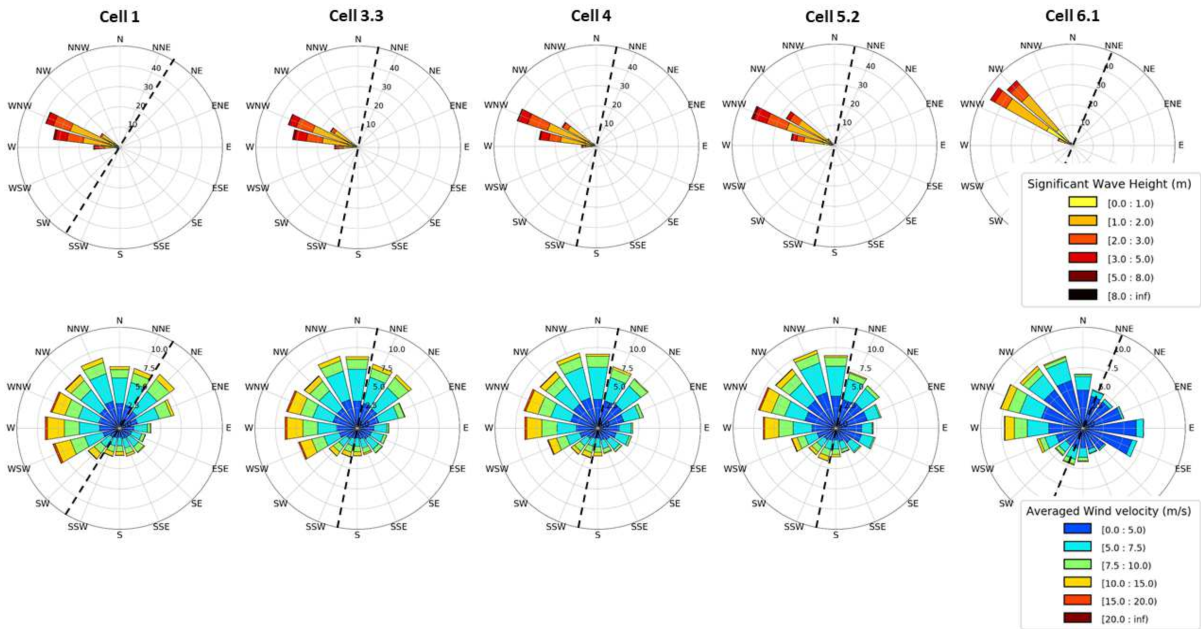

Figure 2: General characteristics of significant wave height and means 10 m-wind conditions along the coast from 2008 – 2018 (hourly hindcast data, see section 2.3). Dashed black lines represent the coastline orientation at each sedimentary cell.

Table 1: Nearshore system and beach-dune main characteristics along the Aquitaine coast

The first line dune along the Aquitaine coast is almost continuous and fixed. The human intervention on the dunes start at the half of the 19th century mainly through the plantation of ammophila arenaria used to stabilize the seafront dune system. Then, the dunes of the Aquitaine coast were progressively fixed, reprofiled and managed by the French National Forest Office ONF in the 1960s. Since then, no significant increase in the erosion rate was observed, which was attributed to the dune management performed by ONF (Castelle et al., 2018). However, the coastline evolution trends are geographically highly variable. Since 1985, coastline retreat rates are evaluated at 3.3 m/year in Nord Medoc (Cell 1) and 0.8 m/year in central Landes (sub-Cell 5.2 or 5.3) in Bernon et al. (2016). Strong variability was also observed at seasonal time scales, such as after the 2013-2014 winter, where field observations show in some areas a more than 25 m coastline retreat and in others no significant impact (Bulteau et al., 2014, Castelle et al., 2015).

2.2 Data

The main sources of data processed in this study are extensive coverage airborne LiDAR campaigns realized by the French National Geographic Institute (IGN) all along the Aquitaine coast. LiDAR campaigns were realized with synchronal orthophotography campaigns with a resolution of approximately 0.1 m. The control for data accuracy was realized in the raw data in which the density can vary between 2 and 8 points/m². LiDAR data were controlled by comparing them with dedicated d-GPS data uniformly distributed along the coast (1550 points in unobstructed and flat surfaces on hard ground, such as parking, sports grounds, and roads). All campaign conformed to typical LiDAR accuracy ranges, with an absolute error of less than 20 cm (Table 2). The analysis presented in the study was realized on the 1 m horizontally gridded DTM in the French official altimetric reference called NGF/IGN69.

Apart from the 2011 campaign, which occurred just after the winter, all other campaigns occurred in the post-summer period and during approximately the same period before winter storm events (Table 2). Therefore, except for the 2011 campaign, beaches will show post-summer characteristics, thereby offering relevant information for interannual comparisons and avoiding seasonal bias.

Table 2: LiDAR campaigns

To complete an in-time LiDAR campaign analysis, data from annual post-winter d-GPS campaigns collected at 55 stations along the whole Aquitaine coast were exploited (Figure 1). Beginning in 2006, the Observatory of the Aquitiane Coast (OCA) (see www.observatoire-cote-aquitaine.fr) has collected topographic transects annually based on a dedicated geodesic network implemented along the coast after the winter and the main storm erosive events. During these surveys, geomorphological descriptions of each profile were made to monitor the apparition or evolutions of incipient foredunes, beach scarps, pioneer vegetation, and evolutions of the frontier between the free dune (also called white dune), the grey dune and the forest.

The location and the spatio-temporal evolution of the coastline is also used to analyze LiDAR data. Many definitions of the coastline can be found in the literature (Boak and Turner 2005). The relevance of one or another depends basically on their applications and the objective of each study. In our case, a practical definition based on geomorphologic criteria is used. The dune foot (Df) is defined as the slope break between the dune front and the upper beach or the foredune. The justifications to use this definition are multiple: (i) it allows an objective and common visual detection on the field, with orthophoto interpretation as automatic detection with GIS treatment (Figure 3), (ii) it enables detecting a limit whose evolution is in line with substantial erosion and recovery processes, (iii) it allows interpretations of seasonal and interannual evolutions.

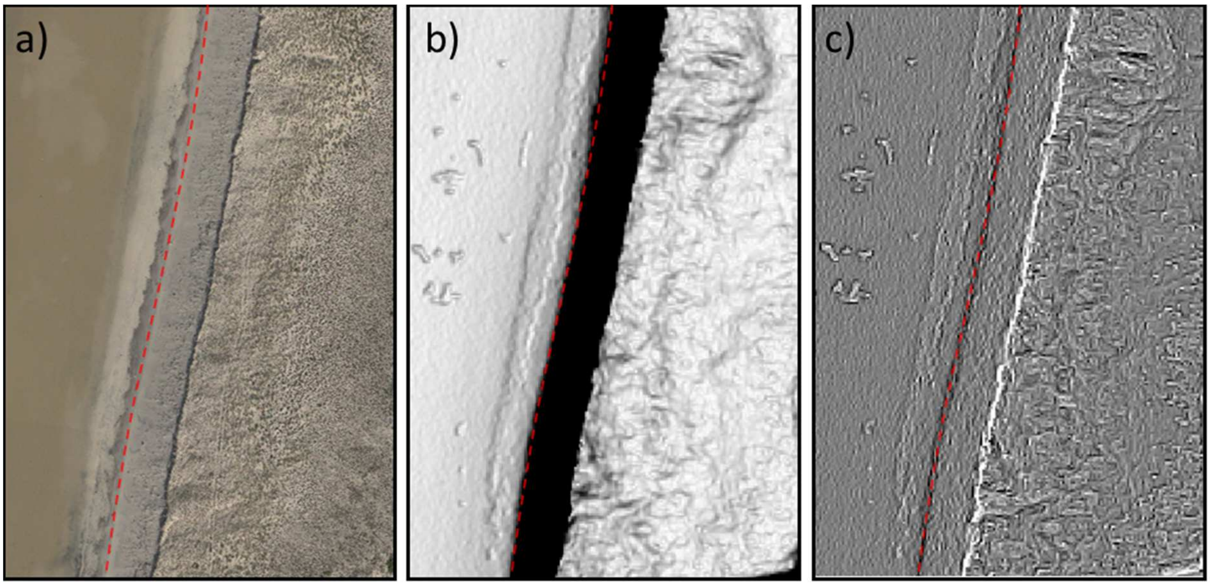

Figure 3: Tools for the dune foot location (dashed red line) as the coastline definition, a) Draped DTM; b) Slope map; c) Longitudinal curvature map.

2.2 LiDAR treatment

2.2.1 Dune scarps, incipient foredune detection and beach-dune sand volume evolution

Part of the analyses are based on a GIS treatment dedicated on the one hand to detect automatically and delimitate massive beach scarps and associated eroded dune areas, and on the other hand, to detect established incipient foredunes directly in contact with the dune front (Figure 4).

Between two LiDAR campaigns, erosion scarps are defined as an altitude loss exceeding 3 m, directly in contact with the dune foot. These values were retained to exclusively consider massive erosion marks where the morphological impact was superior to the annual winter beach lowering (typically approximately 1.5 to 2 m). Several tests evaluated the applicability of lower values (2 m and 2.5 m). With a threshold smaller than 3 m, erosion pattern delimitations are noisier and are longshore-continuous in many parts of the coast, thereby not meeting a satisfactory analysis of erosion intensity. In contrast, incipient foredunes are altitude gains exceeding 1 m in direct contact with the dune foot. Incipient foredunes with inferior characteristics (several tens of centimeters) were not extracted mainly because with an accumulation under 1 m, foredune are hardly detectable on the field and were not considered as thoroughly established. For each kind of landform, a surface threshold of 500 m² is fixed to isolate only significant objects.

The altitude and thresholds used to define each kind of landform were compared and validated with observations taken during annual field campaigns along the coast and were based on synchronal photo interpretations made during the LiDAR campaigns.

Figure 4: Photographs of the erosion dune scarp and foredune installation at the grand Crohot beach (Cell 3.4)

To evaluate the main characteristics of erosion and recovery patterns along the coast, a classification of erosion and recovery is proposed based on their alongshore lengths as follows: Class 1 >800 m long; Class 2 from 400 to 800 m long; Class 3 from 200 to 400 m long; and Class 4 <200 m long.

Additionally, sediment budgets were calculated all along the coast using the dune foot of 2014 as the baseline. The budgets are calculated between 100 m seaward on the beach (near the Mean Sea Level) and 50 m landward on the dune starting from the dune foot (Figure 9). These limits were used to evaluate evolution at the beach-dune interface and limit the role of the intertidal zone variations, which can be substantial even at the tide cycle time scale. Complementary treatments consisting of isolated specific dune and upper beach erosion/accretion were made. On the basis of the differential volume of 2011-2014, the eroded volumes relative to the upper beach and to the dune were identified as being before and after the 2011 coastline, assuming that the coastline retreat observed in 2014 was mainly related to the 2013-2014 winter storm events. The same treatment occurred for the 2014-2017 period in considering the volumes before and after the 2014 coastline.

2.2.2 Cross shore analysis of beach erosion and recovery

On energetic open coasts, if small-scale morphology or sand levels can be highly variable at short time scales (day to weeks), the foredune and dune foot are considered as more established landforms (Hesp 2002) that are affected only during main storm events.

Three altimetric proxies considered in reference to the French topographic datum (NGF-IGN69) are used to characterize the cross shore evolutions of the beach-dune interface, namely, the upper beach/foredune (4 m/NGF), the dune foot (6 m/NGF), and the dune front (10 m/NGF) (Figure 8). The temporal evolution of each proxy is analyzed along 1 km-spaced profiles perpendicular to the coast. This spatial resolution was considered as relevant for a regional scale analysis and is superior to potential periodic erosion marks observed along the coast, such as mega cusps.

The value of 4 m/NGF was retained because it corresponded in the major part of the studied profiles to the front of the incipient foredune, when this type of morphology is established and observable in the field (Figure 8). Due to the alongshore variability of beach slopes, sediment availability, and granulometry, these contour values can also be associated with the upper beach dynamic (erosion or accretion). However, taking into account that 4 m/NGF corresponds to 1 to 1.5 m above Highest

Astronomical Tide level, erosion at these contours should be related to highly energetic marine storm conditions and, conversely, accumulation morphologies are mainly related to wind driven dynamics.

For the dune foot, the value of 6 m/NGF corresponding to the alongshore and interannual average elevations (Nicolae et al., 2018) was used. As previously mentioned, the topography of the beach is variable from north to south, and the dune foot height varies between approximately 5 m at the north (Cell 1 and 2) to approximately 7 m at the south (Cell 6). Dune foot height at a certain location can also vary seasonally, being potentially exposed to winter storm erosion (lowering of the dune foot) and rapid sand accumulation related to favorable north-coming winds (rise of the dune foot). However, 6 m/NGF is meaningful and consistent for characterizing the evolutions of the beach-dune transition along the coast (Figure 8) at interannual and regional scales.

Finally, the dune front proxy located at 10 m/NGF directly characterizes the progradation or the retreat of the dune front all along the coast. Interpreting data just before a massive erosional event evolution of this proxy (typically progradation) can be related to the dune front sliding and slope regularization. This is not the case in our study, surveys having occurred after the summer season.

2.3 Hydrodynamical data

Hindcast hydrodynamic data are analyzed to characterize interannual and spatial variabilities at a seasonal time scale for water levels and wave energy along the coast. These data are currently used in the Aquitaine Early Warning System through synthetic indicators relating local storm surge conditions, wave conditions and geomorphological characteristics of the coast (Nicolae Lerma et al., 2018).

Tide and atmospheric surge data are collected from the MARC platform (Modelling and Analysis for Research in Coastal environment, www.umr-lops.org/marc), and more precisely, from the structured domain covering the whole Aquitaine coast with a spatial resolution (Δd) of 250 m. Data are extracted every 15 min for every 5 kilometers along the coast along the 10 m depth isobaths. The reference datum is the mean sea level (MSL), requiring a spatially variable vertical correction (RAM, 2016) to convert the results into the local topographic datum (IGN69).

Wave data are also extracted from the MARC platform but from an unstructured domain with Δd approximately 200 m at the coast. Data are extracted every 1 h along the 50 m depth isobath in front of the water level extraction point.

Based on hourly data, two time series of daily maximum conditions at the center of the coast are presented in Figure 5. The time series are used here to characterize the relative intensity of the successive winters during the study period and linked the intensity to the erosion and recovery process.

The wave energy flux per length unit of wave crest (noted P) expressed in kW/m (Figure 5) was calculated in deep water according to the following equation (Tucker and Pitt 2001):

$$P = \frac{\rho g^2}{64\pi} TpHs^2$$

where ρ is the density of sea water, 1030 kg/m3; g is the gravitational acceleration, 9.81 m/s²; Hs is the significant wave height; and Tp the peak period

The Total Water Level (TWL) was calculated by summing the tide level, the atmospheric surge and the vertical runup (including wave setup and swash). The runup was estimated using two formulations developed by Stockdon et al. (2006) for intermediate and dissipative beaches. For the intermediate beaches, the slope parameter was set to 0.05 based on the typical mean upper beach profiles observed along the coast (Bulteau et al., 2016).

To illustrate the relative homogeneity of the forcing along the coast, the deviation of TWL for a point at the north (Cell 3.2) and at the south (Cell 5.3) of the coast relatively to TWL at the center of the coast (Cell 4) is illustrated (Figure 5). Differences in *Hs* for the same storm event are rarely above 1.5 m from north to south (not shown). The tide level and atmospheric surge are also quite similar along the open coast (excluding the Arcachon lagoon). Consequently, the variability at the scale of a storm event is reduced by approximately 1 m maximum from north to south (Figure 5). The forcing is thus considered as quite homogenous along the coast, and the alongshore variability of erosive impacts at the beach are mostly related to sediment availability and associated morphological characteristics (nearshore bar system, beach width, beach slope, and dune foot elevation, see Table 1)

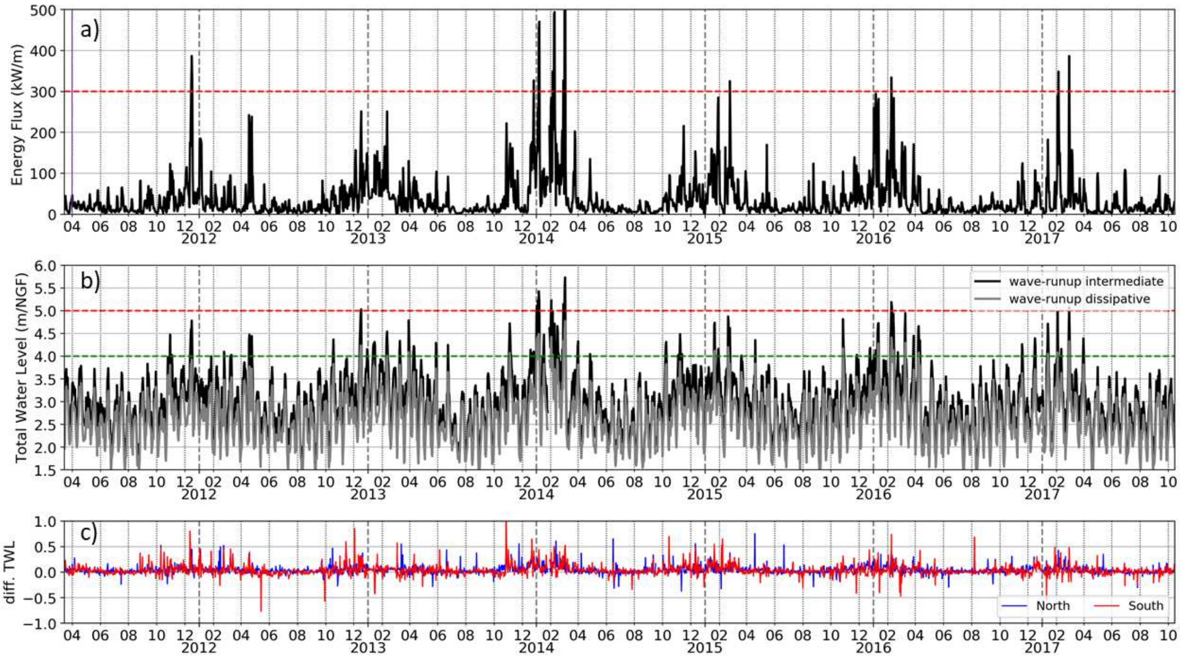

Figure 5: Daily maxima of forcing parameters along the coast between April 2011 and October 2017, horizontal dashed lines represents thresholds in a) intense storm (wave criteria), Bulteau et al., 2019, in b) green dashed line upper beach/foredune proxy, red dashed line lowest dune foot detected along the coast.

3. Results

3.1 Erosion characteristics after the 2013-2014 winter

3.1.1 Dune scarp and beach erosion patterns

The automatic beach scarp detection indicates that almost all the coast was affected by substantial erosion between 2011 and 2014. Along the coast, 255 erosion marks with a surface area above 500 m² were detected along the coast. Erosion marks present variable characteristics between 16 to 3080 m long and 4 to 44 m in width. The width of the erosion pattern was relatively homogenous along the coast (between 11 and 24 m on average). Classification based on the alongshore length criteria was retained, as it was more significant for analyzing the geographic repartition of each type of erosion pattern (Figure 6, Figure 7).

Erosion scarps detected in 2014 show great variability in shape along the coast. Due to a relatively homogenous width, the main criteria used to classify the erosion marks is the alongshore dimension, but erosion marks can also be analyzed in terms of shape (Figure 6). Class 1 characterizes continuous eroded bands with quite homogenous cross-shore widths. This shape is expected to be observed on highly exposed dissipative beaches with uniformly low-gradient intertidal beaches, unpronounced or longshore uniform sand bars and low available sediment resources. The long-eroded bands are mainly observable in North Gironde, where beaches show those characteristics.

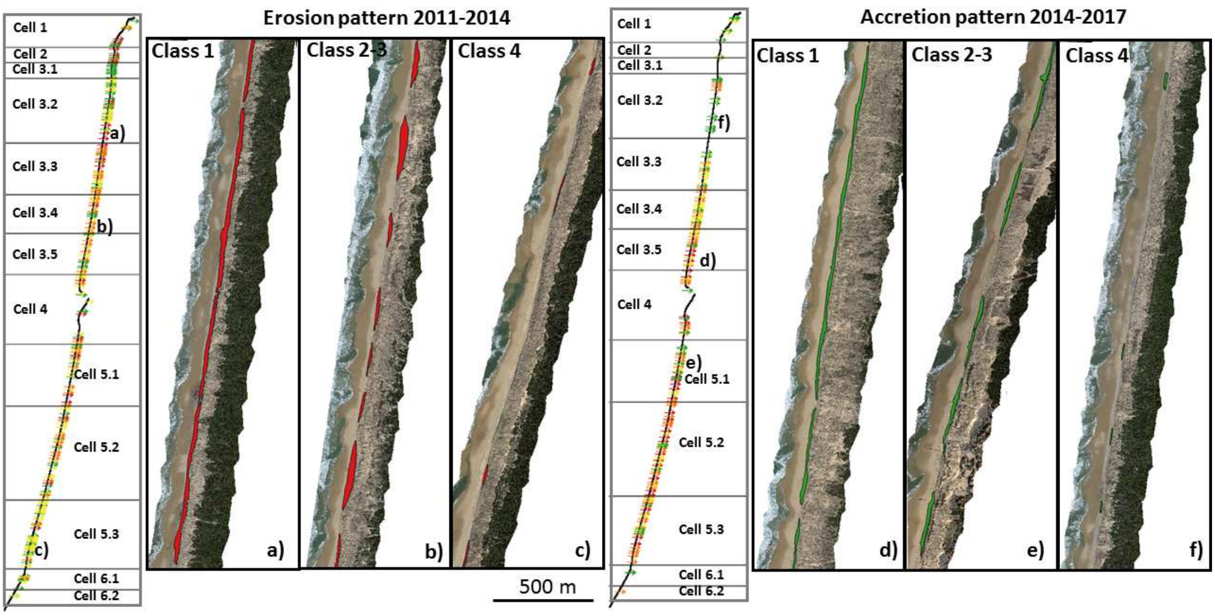

Figure 6: Distribution of eroded dune scarps in 2014 (left panel) and foredunes in 2017 (right panel) and an example of each class along the coast. In maps, crosses indicate erosion/accretion location, red class 1, orange class 2, yellow class 3, green class 4. In orthophotos, red polygon delimits erosion marks (left panel) and green incipient foredune (right panel).

Classes 2 and 3 are cusp-shaped erosion scarps defined as a megacusps embayment (Thornton et al., 2007; Castelle et al., 2015). The geometry of the megacusps are symmetric, with the center of the embayment located roughly equidistant from its horns. The alongshore erosion differences during storms such as mega cusps are related to nearshore bathymetry and particularly so with persistent rip currents channels (Bender & Dean 2003; Schupp et al., 2006; Thornton et al., 2007; Houser et al., 2008, Castelle et al., 2017). Rhythmic mega cusps are observable all along the coast but appear to have a higher alongshore length in central and south Gironde compared to the Landes coast, where they are more generally approximately 200 to 400 m in length (Class 3) (Figure 6). Finally, Class 4 corresponds to local, generally also cusped, erosion marks or little scarps intercalated between the Class 1 shape.

Class 1 represents only 8.6 % of the number of erosional patterns detected but totals 55.6 % off of the dune front eroded area. This pattern is representative of massive erosion, with a maximum of 44 m width localized in Cell 4 at the south end of the Arcachon Lagoon pass. The maximum eroded surface reaches 676 555 m² localized in Cell 2.

In comparison, Classes 2, 3 and 4 respectively total 22.6 %, 16.4 % and 5.4 % of the eroded area. Notably, for each class, the width of the erosion marks can vary from a few meters to more than 30 m. Even if the erosion pattern of Class 4 is relatively small in the longshore direction, the width can be substantial, with an average of 11.8 m and reaching more than 30 m in Cells 1 or 4, for example.

The spatial repartition of each class of erosion pattern is represented in Figure 6 and Figure 7. These figures illustrate that erosional marks are observable all along the coast. We observe that the northern coast's (from Cell 1 to 3.2) erosion marks are mostly characterized by Class 1 and Class 4 patterns. Conversely, the central part of the coast, including the central and south part of the Gironde and Landes coasts (from Cell 3.3 to 5.3) are mostly characterized by Classes 2 and 3. Finally, the extreme south of Landes (Cell 6 and 7) counts fewer erosion marks, and they are mostly from Class 4.

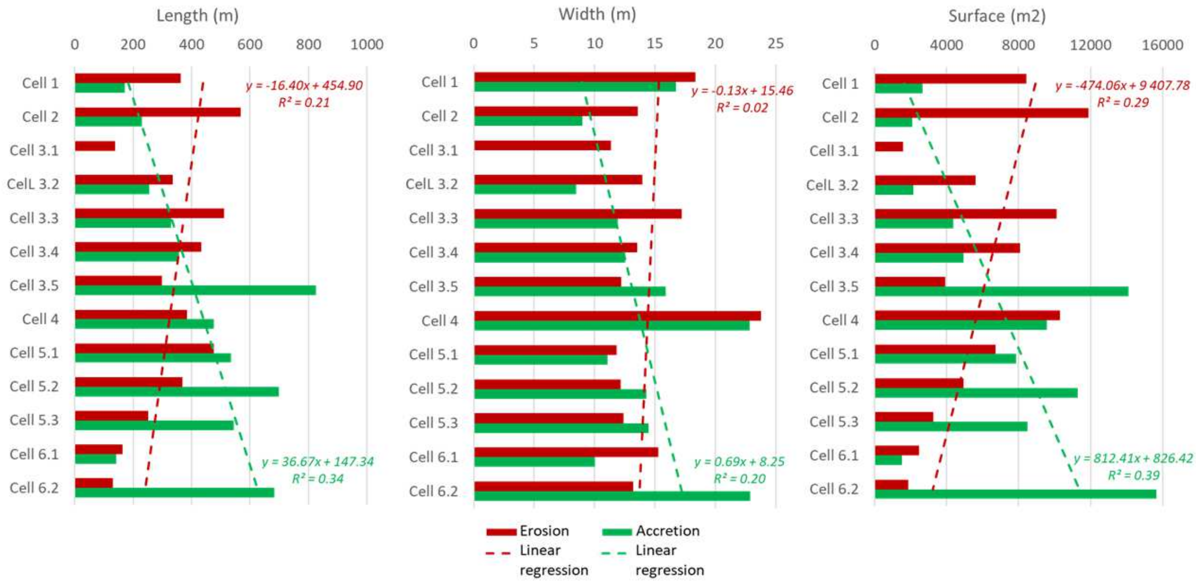

Figure 7: Mean characteristics of dune scarps and accretion patterns along the coast, 2011-2014 period (red bar), 2014-2017 period (green bar).

3.1.2 Cross shore beach-dune interface retreat

The retreat of the beach-dune system was very prominent almost all along the coast, except at the extreme north end of Cell 1, at the direct proximity of the Arcachon inlet and at the extreme south of the Landes (Cell 6.2), where progradation of the Df was observed. However, due to a local singularity due to wave/tide interactions, hook ridge dynamics, or wave expositions, a planimetric retreat was generalized between 5 and 20 m and beach lowering reached more than 2 m. The alongshore average retreat is 6.5 m for the dune foot and 4 m for the dune front. Even if erosion is generalized, a north to south gradient is observable, which is consistent with the previous classification of the erosion marks (Figure 7). This dynamic is particularly observable considering the evolution of the dune front proxy. The north (Cell 1) and the center of Gironde (Cell 3.2 and 3.3) were the most dramatically affected areas, with massive retreats greater than 20 m (Figure 8 and 11). The south end of the Arcachon inlet also observed brutal retreat, but it was much more local. Interestingly, the dune front was relatively preserved in Landes (mostly Cells 5.1 and 5.2). Dune retreat was observed locally at the same order of magnitude as in Gironde, but more generally, the dune front appears stable and some slight progradation is even observable (Figure 8 and 11).

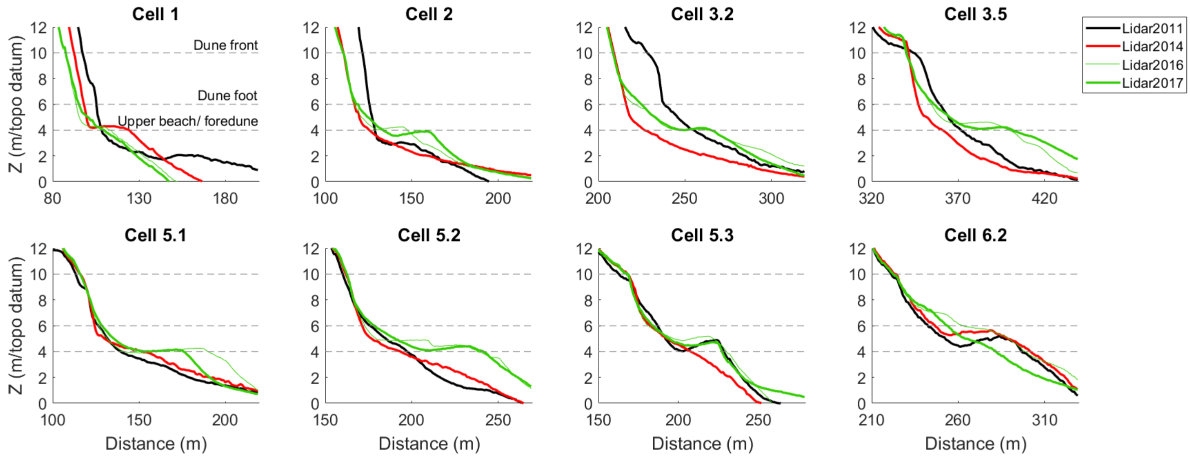

Figure 8: Example of erosion and accretion at the altimetric proxies used in cross shore analysis along the coast

In Landes, the situation in much more contrasted, with many locations presenting at least progradation at the Upper beach/Fordune proxy. This is related to rapid recovery at the upper beach during the month directly after the 2013-2014 winter.

In Cell 6, we observe consolidations of the foredune that have not been significantly affected thanks to the specificities of beach-dune morphologies in this section of the coast (i.e., coastline orientation, coarser sediment, nearshore bar system) (Figure 8 and 11).

3.1.3 Upper beach and dune eroded volumes

Erosion volume at the beach-dune interface was massive along the coast. The only part of the coast not affected by erosion is the extreme south (Cell 6.2), which even benefits from the sediment supply (Figure 9). Along the coast, 71 % of the eroded volumes were taken from the dune front versus 29 % from the upper beach. However, differences are observable from north to south with a significant gradient illustrated by the linear regressions in Figure 9. We observe that the erosion in Cells 1, 2 and 3.1 was almost exclusively related to the dune retreat, and volume eroded from the upper beach represents less than 25 % (Figure 9). For example, in Cell 3.1, 88 % of the eroded volume at the beach-dune interface was taken to the dune. In Cells 3.2, 3.3, 3.4 and 3.5, the situation is more balanced and the eroded volumes at the dunes are comparable to the volumes eroded at the upper beach, showing that massive beach lowering and dune retreat are associated with this part of the coast. Total erosion at the beach-dune interface presents higher values along the coast until 3 165 103 m^3 is reached at Cell 3.3, representing an average erosion of approximately 166 m^3 per linear meter. In Cell 4, 96 % of the volume is eroded to the dune. In Cells 5.1 to 6.1 in Landes, erosion also mainly affects the dunes between 90 to 62 %. Finally, the budget in Cell 6.2 is positive and accretions are mainly localized at the upper beach (85 %).

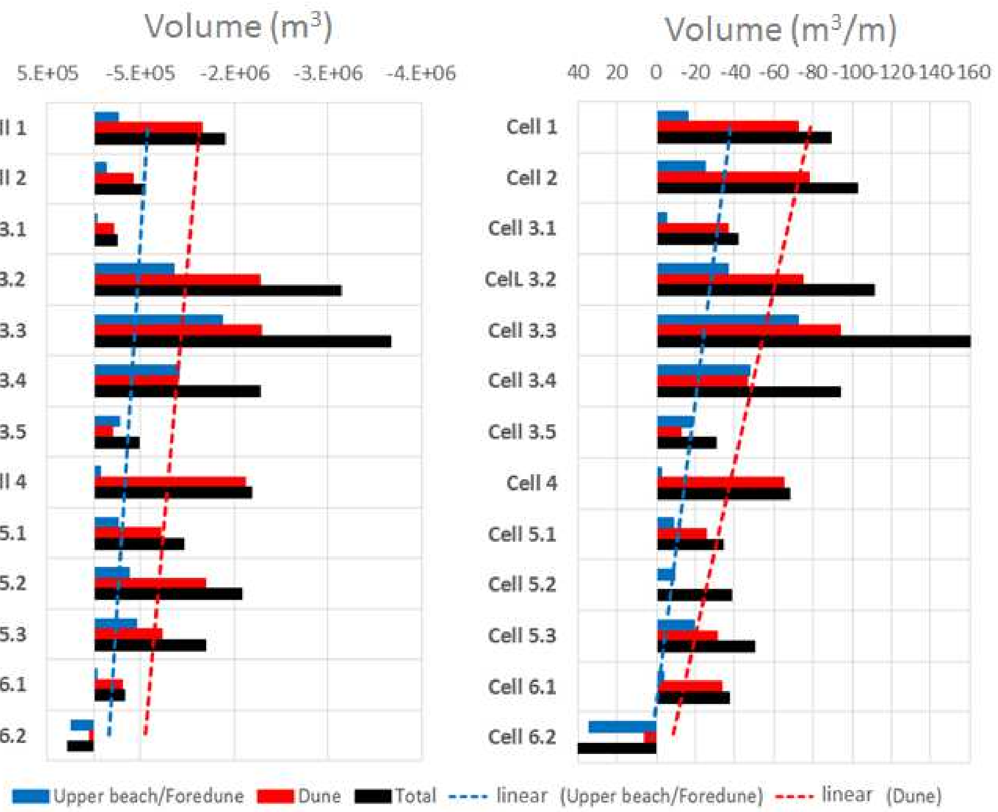

Figure 9: Distribution of the eroded volume along the coast at the beach-dune interface between 2011 and 2014

Even if we can consider that the entire coast was severely affected by beach erosion and dune retreat, we found some substantial geographical differences that are also observable in the following period of recovery in 2014-2017.

3.2. A progressive recovery between during the 2014-2017 period

3.2.1 Incipient Foredune pattern

As well as for erosional patterns, almost all the coast was experiencing the recovery process during 2014-2017 (Figure 7 and 8). In 2017, 188 foredunes with a surface larger than 500 m² were detected relative to the beach-dune state observed in 2014. The main characteristics of these foredunes are between a 30 and 3360 m alongshore length and 4 to 77 m width.

Classes 1 and 2 represent 14.3 % and 33.0 % of the number of recovery marks detected, respectively, and a total of 56.4 % and 30 % of the entire recovery area, respectively. Compared to erosional marks, foredune patterns are generally larger in the alongshore direction. They are also thinner with an average width of 18 m for Class 1 and 15 m for Class 2.

More local recovery marks are also observable in Classes 3 and 4, representing 27.1 and 25.5 % of the total number of recovery marks, respectively. The widest foredune marks are observable in Cell 4 at the spit of Cap Ferret, reaching more than 70 m. This massive accumulation of sand at the dune foot is related to the hook ridge dynamic taking place at the Cap Ferret spit. Interestingly, comparing the sum of the eroded area with the recovery area, only 9.0 % of the eroded area remained in the 2017 survey.

A geographic difference in the foredune pattern is clearly observable along the coast. Class 1, which represents massive and longshore extended foredunes, is only observable in Landes (Cell 5.1, 5.2, and 5.3), except in the south of Gironde close to the Cap Ferret Spit. In Landes, classes 2 and 3 of the foredunes are also observable, showing that foredune constitution is an important process in this part of the coast. Conversely, at the extreme north and south ends of the Aquitaine coast, incipient foredunes are poorly detectable or are only at a local scale (Class 3 and 4). Between the two, the center of the Gironde coast (3.3, 3.4 and 3.5) is mostly characterized by Class 2 and 3 foredune patterns. In Figure 6, the location of the Class 1 erosion form is almost opposite compared to recovery patterns. Locations for Classes 2 and 3 appear consistent, suggesting that foredunes can be promptly detected in previous dune scarp locations as observed by Castelle et al., 2017. Finally, erosion and recovery in Class 4 do not appear to be connected.

3.2.2 Cross shore beach-dune accretion

Between 2014 and 2017, the progradation at the upper beach/foredune proxy was massive and generally observed all along the coast (Figure 11). The progradation was on average approximately 11 m and was greater than 20 m in many locations. The only part of the coast observing a retreat at this proxy are Cells 2, 3.1 and 6.2. Notably, these cells were among the least affected by retreat during 2011-2014. For cells 2 and 3.1 the poor progradation or stability seems to be related to the dynamic observed in 2011-2014 to the specific nature and geology of this part of the coast. Evolution during the erosion and accretion phases at these elevation contours are limited due to paleo soil outcrops. For Cell 6.2, the reasons are less clear and are probably related to beach characteristics and the dominant longshore drift, which moves the sediment from south to north.

The dune foot location was also prograding at the Aquitaine coast scale, with a value of approximately 2.1 m on average along the coast. Cells where the foredunes prograded the most are also those where the dune foot prograded the most (Cells 3.3, 3.5, 5.2 and 5.3). However, along the coast, evolutions at the dune foot can be notably variable with, for example, a mean progradation of approximately 4.6 m and 6.9 m in Cells 3.5 and 5.3, respectively, and a mean retreat of approximately 5.6 m and 0.9 m in Cells 2 and 7, respectively.

As expected, the dune front appears to be much more stable, mainly because recovery processes promoting dune front progradation generally take a longer time, such as several years to decades (Hesp, 2002). However, some slight progressions of the dune front are observable in Landes (Cells 5.1 and 5.2) indicating a sand supply movement from the beach to the dune. This progradation can be significant, locally reaching 5 m to 8 m, and Cell 5.1 and Cell 5.2 are approximately 0.4 m on average. Conversely, the dune fronts in Gironde are mostly retreating (except locally in Cell 3.4). The retreat is on average greater than 2 m in Cell 1 and Cell 6, approximately 1.8 m in Cell 2 and approximately 1.3 m in Cells 3.3, 3.4, and 3.5. This retreat is concomitant with a general accretion observable at the dune foot, which denotes an erosion sequence occurring during winters of the 2014-2017 period (discussed in section 4.2).

3.2.3 Volume recovery at the upper beach and dune interface

Between 2014 and 2017, the gain in volume at the beach-dune interface was massive and was localized at 90 % of the upper beach. Dune erosion occurring during the winter of 2013-2014 are observable in Cells 1, 2, 3, 4 and 6, and accretion is mainly observable at the upper beach. Along Cells 3.5 and 5, accretion is massively observed on the beach (between 88 and 98 %) but also benefits to the dune front, which is consistent with the progradation showed by the dune front proxy (Figure 10). The volume stored in the automatically detected foredune pattern (Figure 6) represents only 13.5 % of the total recovered volume, which indicates that most of the sand volumes recovered in 2017 are localized on the upper beach and do not yet constitute established foredunes. This situation, which is prone to the continuation of the recovery process is fragile, however, with the sand accumulated in the upper beach being potentially remobilized during the following winters.

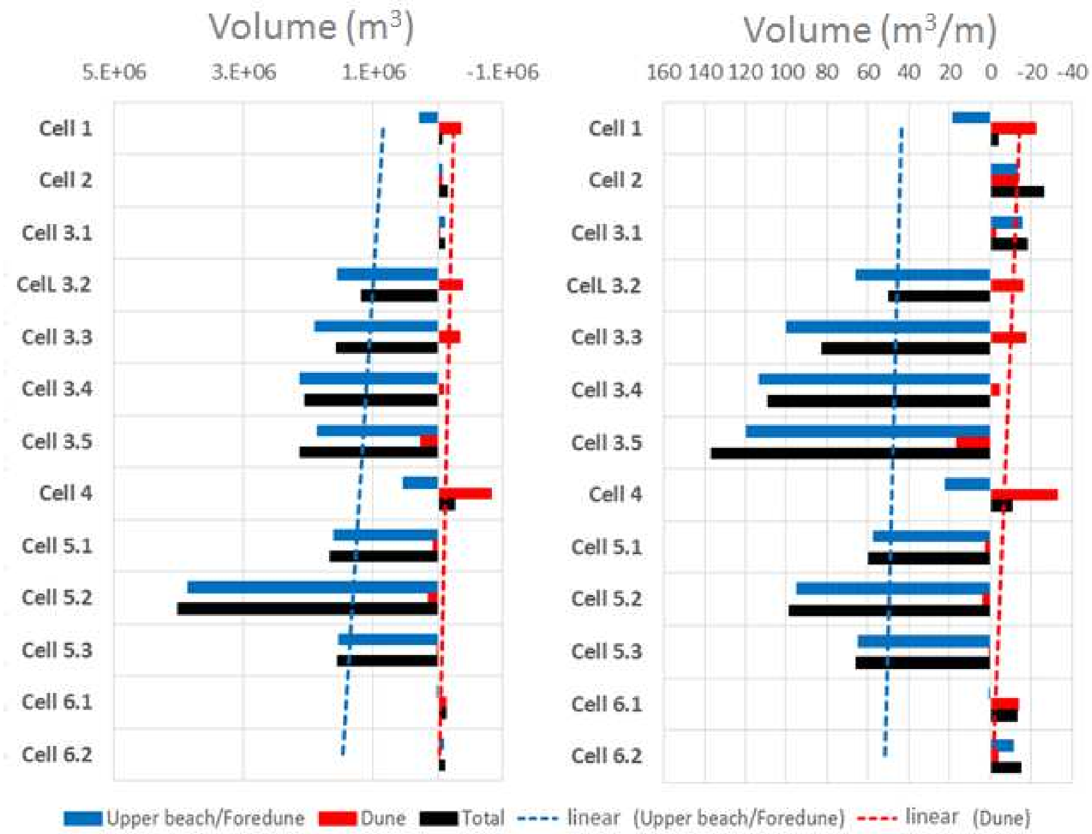

Figure 10: Distribution of the recovered volume along the coast at the beach-dune interface between 2014 and 2017

3.3 Erosion and recovery balance and sediment budget

3.3.1 Planimetric evolution of the beach-dune interface (2011-2017)

Previously, erosion and recovery were analyzed through two distinct periods; here, the difference in the beach-dune state is regarded for the entire period (2011-2017), Figure 11.

Proxy results show that at the Upper dune/Foredune proxy, beaches have globally prograded since 2011 (+7.2 m). However, in northern (Cells 1 and 2) and central Gironde (Cell 3.2), no foredunes are observable, or at least not as many are observable as in 2011. In the dune foot and the dune front, a quite clear north-south gradient is observable (Figure 7).

In Gironde, even if some recovery is noticeable after 2014, the sand supply and accumulation were not sufficient at the dune foot and at the dune front to recover position before the 2013-2014 winter. In 2017, dune fronts still present a retreat between 2 m and 10 m compared to 2011.

Cell 4, being at the direct proximity of the tidal inlet of Arcachon lagoon, is submitted to a specific evolution process and some local instability of the coastline can trigger a massive retreat or progradation at the annual time scale. However, the trend indicates substantial erosion on average during the 2011-2017 period.

In Landes (Cell 5), the situation is different. With a few exceptions along the coast, the upper beach/foredune was significantly prograding at approximately 11.7 m on average, and the dune foot as well as dune front appears to be quite stable between 2011 and 2017 (Figure 11). Even if erosion marks were observable in 2014, a substantial sand supply compensated for losses in many locations. Cell 5.2 has an almost stable balance with retreats between 2011 and 2017 of only approximately 0.8 and 0.7 for the dune foot and the dune front, respectively. In Cell 5.3, the balance is also nearly stable at the dune foot (-0.5 m) but is clearly negative for the dune front (-4.1 m).

At the extreme south of Landes (Cells 6.1 and 6.2), the situation is contrasted; Cell 6.1 presents a notably negative balance at the dune front (-7.1 m) and Cell 6.2 is positive (+1 m).

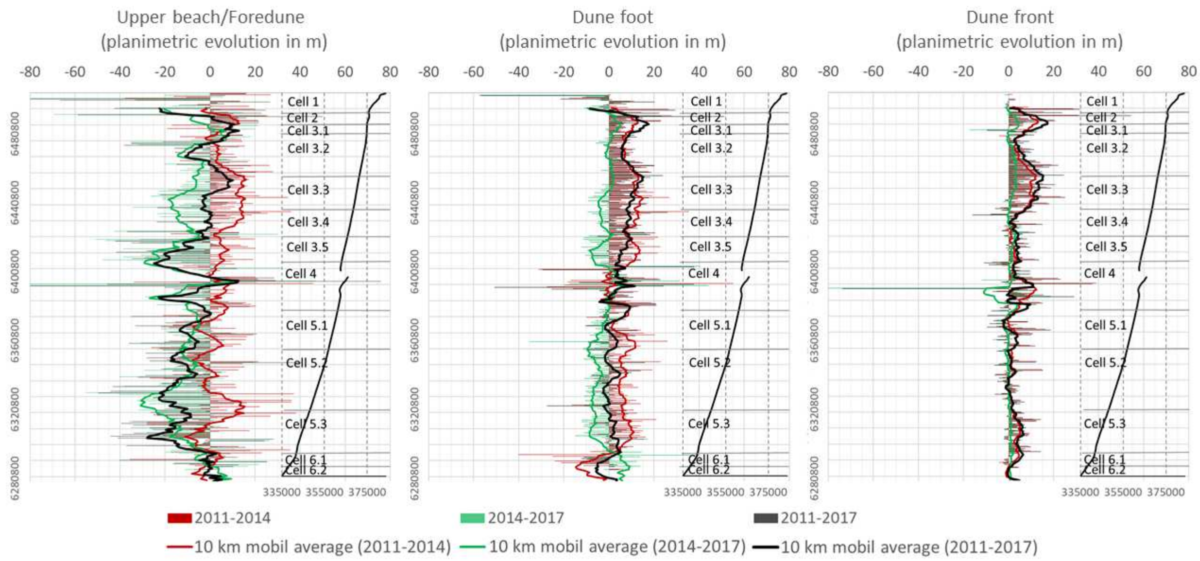

Figure 11: Planimetric differences between 2011 and 2017 at the foredune, the dune foot and the front dune proxies. The black line on the right-sides of each panel represent (plan view of the shoreline).

3.3.2 Sedimentary budget

Consistent with the other analyses, we observe that beach and dune systems have dramatically lost sand between 2011 and 2014, mainly because of the extremely active 2013-2014 winter (Figure 5). More than 15 500× 10^3 m^3 have left the beach-dune interface during this period, which represents an average loss of 66 m^3 per linear meter. The gains during the following period (2014-2017) are also massive and concern almost all the coast. Apart from Cell 5.1 directly downstream of the Arcachon inlet, the parts of the coast still presenting erosion were the extreme north and south. In total, the accretion was larger than 13 500 × 10^3 m^3 with an average gain of 57 m^3 per linear meter.

Considering the total budget between the two periods, 86.5 % of the sand eroded at the beach-dune interface in 2014 returned to the beach-dune interface in 2017. Interestingly, we observe that the sediment that moved to the subaerial system follows the north-south dominant longshore drift (Figure 11). If we consider sub-Cells 3.1 to 3.5 and 5.1 to 5.3, we observe that sand volumes have migrated downstream. This process was generally characterized by a greater amount arriving at the contiguous downstream subcell (Figure 10).

If Cell 1 is excluded from the budget due to its singular characteristics and dynamics at the scale of the Aquitaine coast (divergent longshore drift direction, source of sediment, the urbanization of the coast, dune structuration, and presence of paleo soil outcrops), then only 7 % of the eroded volume has not returned to the beach-dune interface.

In the center of Gironde (Cells 3.2, 3.3, 3.4 and 3.5), a massive sand supply during 2014-2017 is partly compensating for sediment losses that occurred in 2014 (Figure 12). However, the balance is negative for Cells 3.2 and 3.3, whereas it appears positive in Cells 3.4 and 3.5 even if the dune front has strongly retreated in some locations. This can be explained by the eroded volumes in 2014 following a north-south gradient (Figure 9), thus affecting Cells 3.2 and 3.3 more substantially than Cells 3.4 and 3.5. Furthermore, at the beginning of the north-south oriented longshore drift (Cells 2 and 3.1), sediments are rarely available due to no significant natural sand supply source in the system from the north and limited stocks directly on the beach (paleo soil outcrop). The only significant source of sediment in this part of the coast is the eroded sand from the dune fronts.

The downstream subcells 3.4 and 3.5 benefit from a massive sediment supply, but even if the sediments massively returned to the beach-dune interface, the dune fronts have not clearly prograded and are still in their positions reached after the 2013-2014 winter. The sand recovered in this part of the coast is mainly stored in the upper beach and in some incipient foredunes. The recovery process should be considered as partial because in this position sediments can be more easily removed during storm energetic events.

The Landes coast has massively recovered sand, benefiting many dune front locations. For example, in Cell 5.2 the balance between 2011 and 2017 is notably positive with an average gain of approximately 62 m^3 per linear meter (Figure 12). The situation is more contrasted in southern Landes, with Cell 6.1 having substantial erosion during the two consecutive periods and Cell 6.2 surprisingly showing erosion during 2014-2017, despite undergoing gains during 2011-2014. This opposite dynamic can be explained by the specific orientation of the coast. Longshore drift in this part of the coast can be unstable depending on the incoming wave orientation, particularly during storm erosive events, and can explain the contrasted evolution observed in 2014. Conversely, the results in 2017 suggest that a south-north longshore drift is dominating, damaging Cell 6.2.

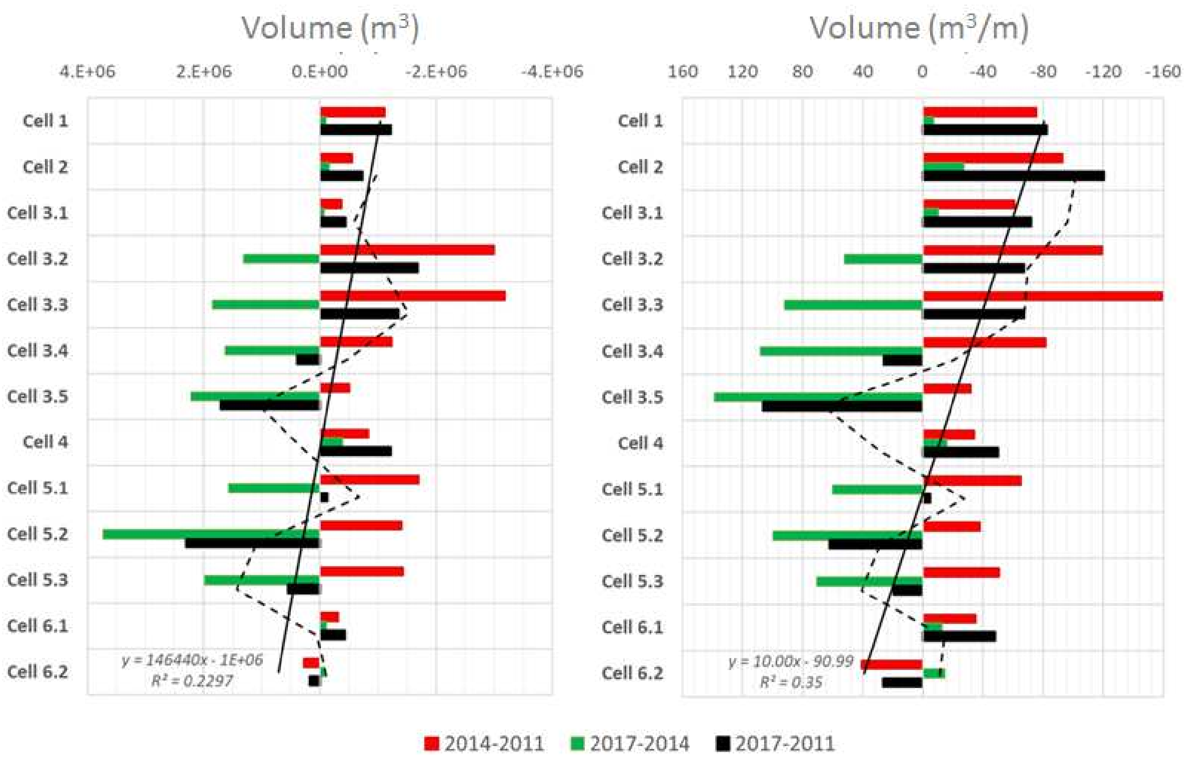

Figure 12: Sediment budget along the coast at the beach-dune interface between 2011 and 2017. Left panel is total m³ and right panel is in m³/m. The black dashed line is a mobile average curve of 2011-2017 evolutions

3.3.3 Pluriannual trends

The previous treatment has shown that the beach-dune interface evolution presents highly variable trends along the coast during 2011-2014 as well as 2014-2017.

Globally, the situation is at a progressive reconstruction of the sand stocks from the nearshore to the beach dune system. However, some cells are following other trajectories. To illustrate those various trajectories at the decadal scale, the analysis during the 2011-2017 period is completed by d-GPS data since 2006. Additionally, pluridecadal trends based on historical photography analysis since 1985 and DSAS treatment (Bernon et al., 2016) are applied to the last decade's evolutions. To be consistent, the dune foot location (Df, cf. section 2.1) is considered for the three datasets. For the illustration, the long-term trend goes back to 1985, but it is shown with 2006 as a reference starting point. The rates of erosion determined at pluriannual (including an extremely energetic winter), decadal and pluridecadal scales are then compared in Table 3 and Figure 13.

Table 3: Rate of coastline evolution along the Aquitaine coast at pluri-annual, decadal and pluri-decadal time scales

We generally observe a quite strong consistency between the three methods and the three periods (Figure 13). Apart from Cell 1, where local erosions are massive and are partly influenced by coastal structures and Cell 2, where the discrepancy between LiDAR and d-GPS measurement is basically due to the number of surveyed profiles (only one), results obtained from the d-GPS network and the LiDAR analysis present similar rates of evolution for each cell. This suggests that parts of Cells 1 and 2 were more contrasted due to local specificities; the OCA d-GPS network gives valuable and representative information about the trend of evolution for each sedimentary cell.

For the rate of erosion, we observe that during the last decade, the dune retreat trends in Cells 1 and 2 are notably faster than expected in pluridecadal analysis (Bernon et al., 2016). D-GPS and LiDAR data show a fast and continuous erosion close to mean pluridecadal trend and a standard deviation during the last decade. In Cell 2, rates are slower, but the tendency during the last decade is higher than the pluridecadal trend. Furthermore, LiDAR data show even faster rates during the final years due to no significant recovery occurring since 2014.

Interestingly, for Cells 3, 4, and 5, the very similar rates obtained by d-GPS and LiDAR show that the erosion in the last decade was slower than the rhythm observed since 1985, which is generally near a trend of less than a standard deviation. In Cell 6, all the trends are consistent and show that Cell 6 and Cell 2 present similar dynamics of erosion during the last decade and are the second most affected sections along the coast after Cell 1.

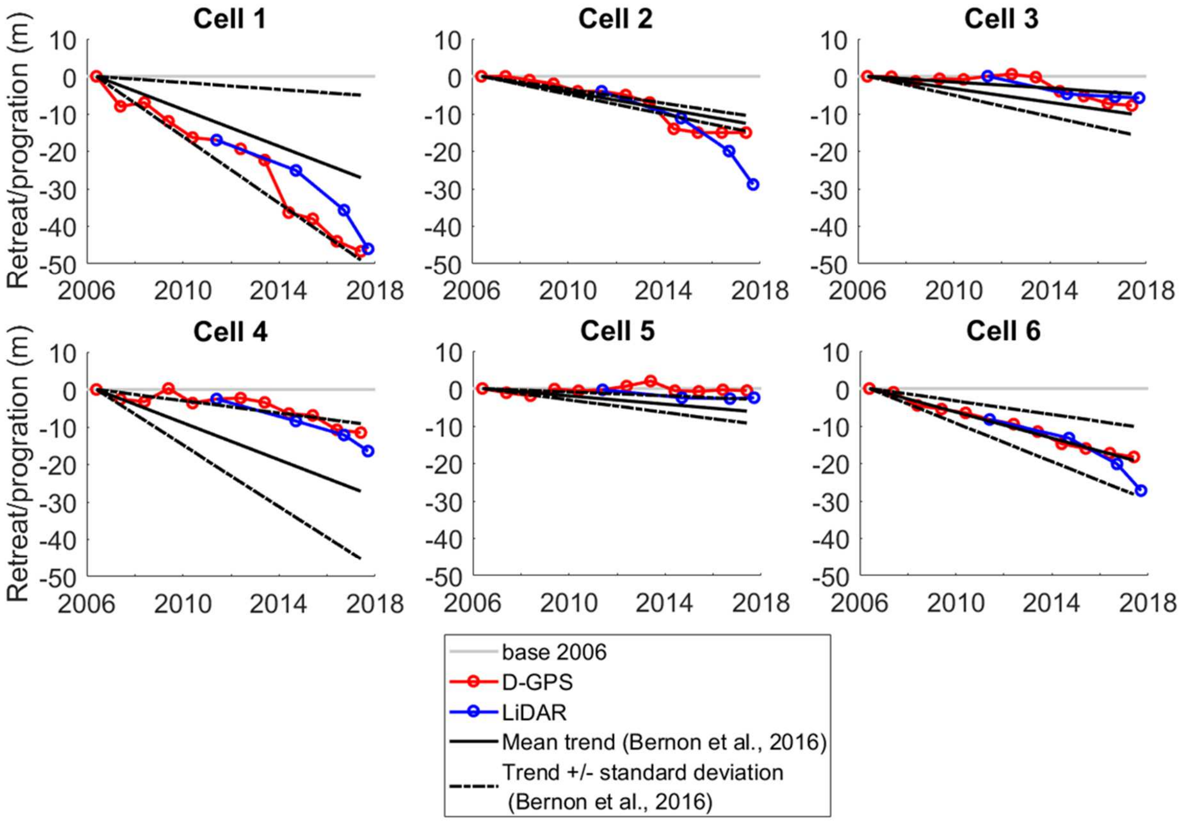

Figure 13: Comparison of erosion trajectories for sedimentary Cells at interannual, decadal and pluridecadal scales

4 Discussion

4.1 Beach-dune evolutions at an interannual resolution

First, topographic measurements such as LiDAR surveys are snapshots of beach states. That implies that the interannual evolution of the beach-dune integrates many successive changes and should be interpreted with caution. This is especially the case when an analysis of pluriannual evolutions is done, whereas LiDAR surveys occur at various seasons of the year. In these conditions, differential analyses can be biased considering, for example, pre- and post-winter beach states.

In our study, LiDAR surveys occurred mostly during the same period of the year, after the summer season and just before the beginning of winter. The only discordant survey was made in 2011 before summer. In other words, the comparison between 2011 and 2014 includes that beach-dune systems in 2011 are marked by the winter state of the profiles (i.e., low intertidal beach and potentially eroded foredunes).

Conversely, the 2014 survey was made after summer, which means this campaign integrates the seasonal summer evolution just after the 2013-2014 winter storms. Castelle et al., 2017 illustrated that some locations along the coast, similar to those in Truc Vert beach, have experienced a noticeable recovery during the 2014 summer. This recovery is characterized by the installation of an incipient foredune at the contact of the dune foot, with some pioneer vegetation installation. However, it takes one more year (Autumn 2015) to observe the installation of a substantial foredune. This local observation is consistent with our analysis, which shows that at the Upper beach/Foredune altimetric proxy (Figure 8 and 11) some parts of the coast (South Gironde and Landes) have already recovered a configuration nearly comparable to 2011 in Autumn 2014. However, in sections of the coast that were massively eroded during the 2013-2014 winter (like north and center Gironde), the beach-dune interface appears highly impacted even after the summer season. Furthermore, the foredune pattern detection indicates only a small number of foredunes between the 2011 and 2014 surveys. Those incipient foredunes are only detected at the extreme north of Cell 1 (banc Saint Nicolas), locally at the south of the Arcachon inlet and along the Landes coast (Cells 5.1, 5.2, 5.3). This indicates that recovery surely occurred at the upper beach, whereas foredunes were still low or nonexistent along the coast after the 2014 summer.

Considering that the urbanized coastline in the sandy Aquitaine coast is very local (representing less than 10 % of the total coastline), the analysis of erosion processes taking place directly around the urbanized coastline is not integrated in this study. However, after the 2013-2014 winter and at an annual frequency, beach management actions, including beach nourishment, sand removal upstream from the drift, beach reshaping or dune stabilization occur along the coast. These actions take place along or near the urbanized coastline and are at volumes of generally approximately 50×10^3 m^3 or less. The supply or modification of the sediment transit along the coast are expected to have impacts only at a local scale and have no significant effect on the analysis at the regional scale. This observation must be balanced concerning Cell 6, where the results can be influenced by the large Capbreton groin and the annual artificial bypass action.

4.2 Sediment availability and recovery process

The beach profile evolutions and the cells and subcells' sediment budgets analyzed previously suggest that during the successive storms of the 2013-2014 winter, most of the sediments eroded on the beach-dune interface were moved to the subtidal beach by cross-shore dominant processes (Castelle *et al.,* 2015). Unfortunately, no bathymetric data are available to support this hypothesis and teledetection-based analysis of the bar configuration or estimating the sediment volume of the nearshore area are not in the scope of this study. However, because (i) currently, no significant amount sand is supplied by the rivers (Gironde, Leyre or the small rivers of the Landes); and (ii) in many parts of the coast, beach have quickly and continuously recovered sediment (in the first month following the winter and over several years). Therefore, most parts of the eroded sediment have likely remained within the nearshore system, being stored on the subtidal beaches.

Previous estimation of chronical loss related to coastline retreat in Gironde coast where approximate at between -15 m^3/m/yr and -20 m^3/m/yr (Aubié and Tastet, 2000). Our results show significantly weaker average loss in Gironde -6.7 m^3/m/yr on the 2011-2017 period and finally stable to positive sediment budget in Landes with gain about 1.6 m^3/m/yr. The sediment budget for all the coast between 2011 and 2017 shows a deficit of $2\,000 \times 10^3$ m^3. It is uncertain that these sediments can be mobilized and return to the beach-dune interface. If we refer to the estimations of Aubié and Tastet (2000), 600 to 900 m^3/yr would be likely to leave the system by migrating offshore in response to sea level rise. They suggest that this amount of sediment would be deposited offshore beyond the depth of closure. Considering that response of sea level rise should be similar along the all Aquitaine coast these estimations look overestimated compared to the results obtained. Our results are more in line with findings of Bellessort and Mignot (1987) which found loss related to sea level rise to between 200 and 300 m^3/yr. However, if the effects of sea-level rise are likely to be responsible for a part of this sediment migration, the dynamics of the currents associated to the extreme storms of winter 2013-2014 also played a role in this offshore migrations.

Between 2014-2017, an overall pluriannual tendency of recovery is observed. Winters during this period were variably intense but are generally low to moderately energetic. During only a few events, TWL barely reached 5 m/NGF (Figure 5), thereby preventing a major part of the coast from experiencing incipient foredune dismantlement. The dune scarp and associate erosion detected during this period indicate that the coast was affected in a significant number of locations (52 in total). However, the length of those eroded areas were mostly lower than 400 m (Classes 3 and 4), and the only part of the coast significantly affected during the winters of the 2014-2017 period was northern Gironde (Cell 1 and 2, 3.2), where two erosion scarps of Class 1 were detected and the dune front has retreated between 5 and 10 m.

More generally along the coast, benefiting from moderately energetic winters and available sediment in the nearshore area, sand has massively recolonized the upper beach, being driven by a mix of marine and aeolian driven processes. The parts of each dynamic at this spatial and temporal scale benefiting at the upper beach appear unclear (4 m/NGF contour). However, at contours higher than 5 m/NGF (and thus at the dune foot proxy), sediments are more obviously supplied by aeolian processes. Consistently, automatically detected foredunes that are in contact with the dune foot generally exhibit more longshore extended dimensions than erosion patterns as related to zonal and longshore homogenous aeolian processes.

Analysis of wind sector distributions indicate that the 2014 – 2017 period was favorable to foredune accretion relative to general wind characteristics (Figure 2) and to the previous period (Figure 14). An average 10 m wind distribution at the center of the coast (Cell 4), which is quite similar to along the coast, is presented (Figure 14). The most constructive winds (NNW to N > 5 $m.s^{-1}$) which represents in annual average around 10 % of the total winds are overrepresented during the period. They exceed 13 % between 06/2015-06/2016 and 15 % between 06/2016-06/2017. The recovery sequence was thus both allowed by moderately energetic winters and rather favorable winds during springs and summers.

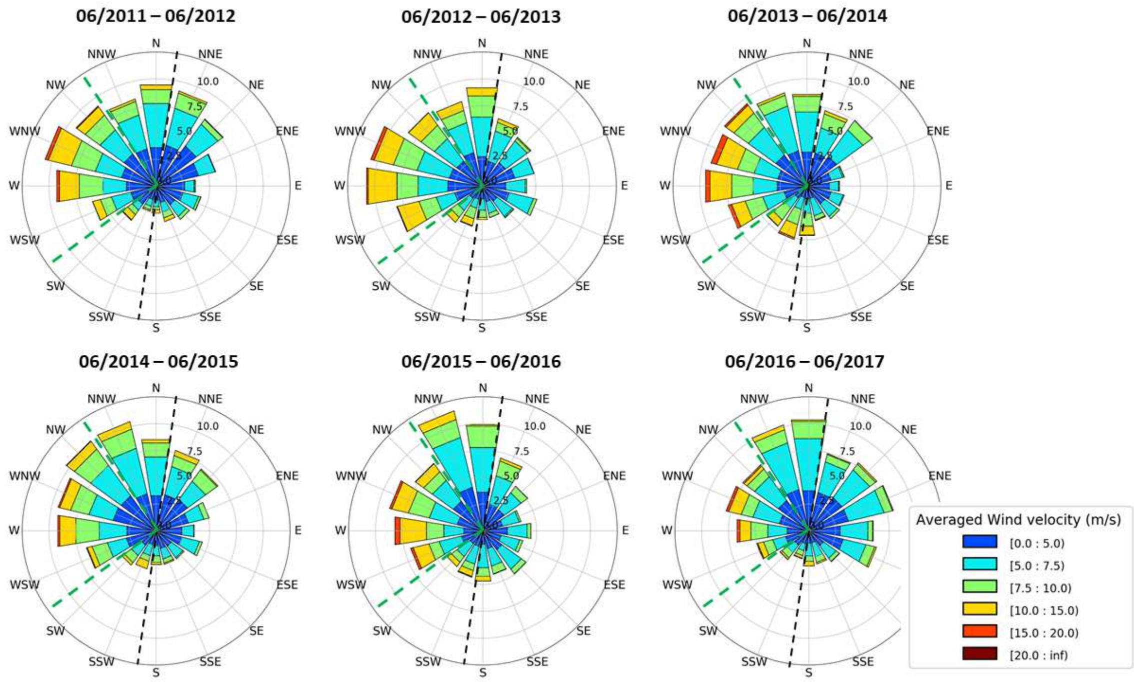

Figure 14: Annual wind characteristics at the Cell 4 during the studied period. Dashed black lines represent the coastline orientation at each sedimentary cell and the green dotted line delimits a more favorable wind orientation for foredune accretion (from north and southwest)

4.3 Beach-dune recovery stages

Erosion patterns at the beach-dune interface are caused by hydrodynamic conditions (water level and wave characteristics) and their dimensions depend on the preexistent nearshore and intertidal beach morphology. Conversely, foredune installation is mainly an aeolian process that on relatively straight coasts is likely to be more homogenous in the alongshore direction. The recovery process related to the foredune installation, dune foot rise and sand migration to the dune front, is much slower than the erosion process, generally taking several years.

If the coast has mainly recovered since 2014, then this trend is not homogenous and follows a variable rate depending on the cells. This leads to variable morphological evolutions observed along the coast. These evolutions of the beach-dune profile can be synthetized as follows (Figure 15):

Stage 1, "massive storm erosion", is the configuration observed directly after a winter that has caused massive beach erosion and dune front retreat. This situation can be extended in time or be accentuated when the beach is affected by a chronical erosion. Along the Aquitaine coast, this case is observable mainly in Cells 1, 2 and 3.1, where interannual recovery processes are generally not observable and beaches are permanently characterized by eroded profiles.

Stage 2, "upper beach recovery", represents the recovery of the upper part of the beach. This situation can be observed a few months after the erosive events in the case of sediment availability, calm marine conditions and favorable winds (moderate intensity northward winds in the Aquitaine coast). After several years, this situation is characteristic of a weak potential for recovery of the system due to low sediment availability and regular erosion even during moderate storms. This situation is locally observable in some parts of Cells 2, 3.1 and northern Cell 3.2.

Stage 3, "incipient foredune growth", shows the constitution of an incipient foredune that can to some extent recover the planimetric position of the beach profile before the erosive sequence. Castelle et al., 2017, based on regular d-GPS surveys, showed that this situation was observable a year and a half after winter 2013-2014 in the south of Gironde (Cell 3.5). After 3 years, Cells 3.2 and 3.3 present this kind of profile, illustrating a slower recovery process at the center of Gironde, which is probably due to a lack of sediment available in the subtidal and intertidal beaches and a southward migration of the sediment eroded during the 2013-2014 winter.

Stage 4, "full beach recovery", is characteristic of recovering beaches where sediments are available on the subtidal and intertidal beaches. Aaeolian processes are actively moving sand to the dune foot and pioneer vegetation is installed at the foredune, thus facilitating sand deposits. The slope break characterizing the dune foot tends to be smoothed and raised. This configuration after three years of relatively calm storm activity globally follows the rate evocated by several authors (e.g., Ollerhead et al., 2013, Houser et al., 2015), who suggest that massive erosion on dunes whose height is greater than 10 m takes several decades to fully recover considering the shape, position and volume. Even if the situation is prone to promote an acceleration of the sand accumulation thanks to the installation and the development of the back shore vegetation in this recovery step (Hesp 2002; Houser et al. 2015), the recovery process remains fragile. Energetic storms can destabilize the recovery process, causing new beach scarps and affecting the vegetation. This kind of profile is observable in Cells 3.4 and 3.5 and more commonly in Cells 5.1, 5.2 and 5.3.

Stage 5, "beach-dune recovery", is observable mainly in the Landes coast, where after the 2013-2014 winter, the beach digging was significantly less important compared to the Gironde coast and where no major erosion was observed at the dune front. In this case, sediment returning to the beach and the backshore benefits the dune, generating a continuous sand ramp from the dune foot to the dune front (Figure 15). The dune foot is still elevating, and the slope break is not clearly detectable. Sand is then accumulated at the dune front. With a massive sediment supply, a new incipient foredune can also appear. This kind of evolution is observable mostly in the Landes coast (particularly Cells 5.1 and 5.2).

Stage 6, "Beach-dune progradation", a few profiles presenting dune front progradation and sand accumulation at the dune crest are observable in Landes. They are mainly localized where erosive impacts during the winter 2013-2014 were very low or limited at the intertidal beach. They present a progressive accumulation of sand on the dune front since 2011 leading to a reduction of the dune front slope and an elevation of the dune crest. Dune crest evolution were generally important between 2011-2014 (approximately 2 m) and then a more progressive accretion occurred between 2014-2017. These differences in elevation rates suggest, in accordance with Hesp, 2002, that dune crest accretion for steep and high dunes (approximately 20 m) is mostly generated by strong winds. This can be an explanation of the relatively few changes of the dune crest during 2014-2017 in comparison with 2011-2014 mainly because of low energy winters.

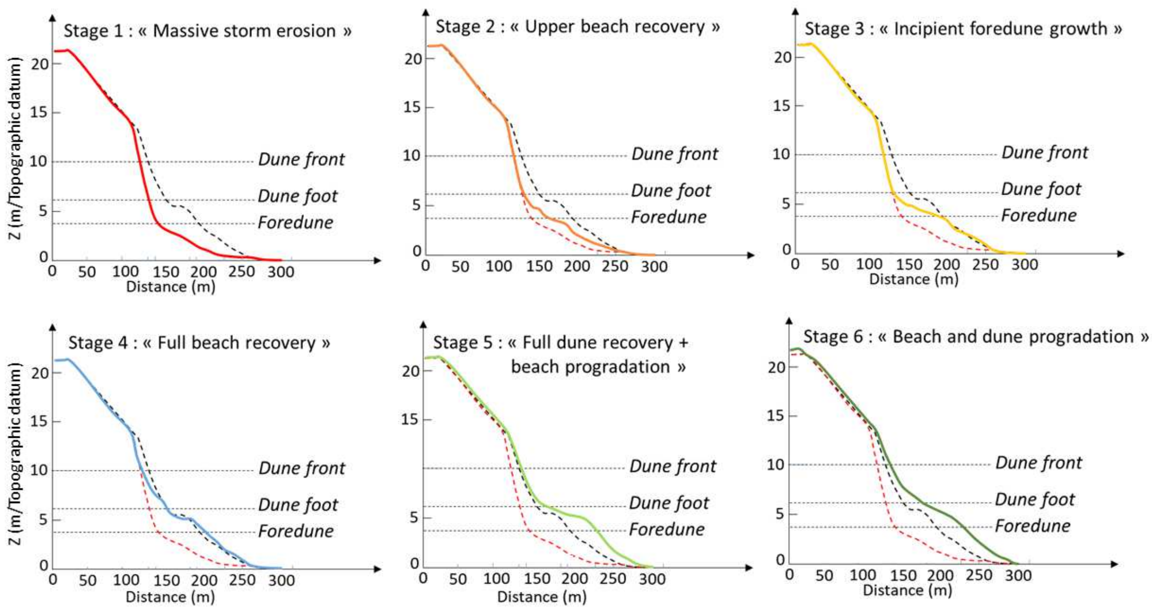

Figure 15: Schematic recovery stages observed along the Aquitaine coast. The black and the red dashed lines indicate the pre-/post-erosive sequence profiles respectively

The presented conceptual evolution based on the observations of cross-shore profile behaviors along the coast is mainly valuable for sandy open coasts. The dynamic at Cell 1 is characterized by chronic erosion and a nearshore environment constituted by submarine rocky platforms and paleo soil outcrops at the dune foot. These singular conditions along the Aquitaine coast prevent us from including this part of the coast in the previous classification. At Cell 4 and mostly at the south of the Arcachon inlet, the direct proximity of the tidal inlet and the sand banks generate a complex and local evolution. Foredunes and dunes are much more unstable, generating a local progradation or retreat at a short time scale as observed in Figure 11. Finally, the beach-dune morphologies and behavior at the south of Landes (Cell 6) are different, which is mainly due to coarser sediment. Beach slopes are steeper, exhibiting successive berms, and dunes are lower. Aeolian dynamics are comparatively reduced due to coarser sediments and the limited width of the potential dry beach.

5. Conclusion

A method coupling a GIS automatic detection of dune scarps and incipient foredunes, a cross-shore morphometric indicators analysis and a sediment budget was applied to analyze erosion and recovery processes at a regional scale. The three approaches appear complementary and give consistent results.

Between 2011 and 2014, particularly after 2013-2014, which was the most energetic winter since 1948, erosion marks were generalized along the coast and are qualitatively linked with typical nearshore bar configurations, intertidal beach heights and the beach width. Erosion marks were classified in several classes, including a highly homogenous longshore erosion band (>1 km length), mega cusps of variable alongshore lengths (from 200 to 800 m) and local erosion marks. A clear north to south gradient was observed for eroded surfaces, volume losses and dune front retreats. The opposite recovery processes, which have taken place since 2014, are generally more marked from south to north, leading to a clearly contrasted trajectory in term of coastline evolutions.

In Gironde, the northern cells present chronic erosion between 2011 and 2017 related to massive erosion characterized by a longshore uniform mark, and no recovery is observable during the 2014-2017. In central and south Gironde, the major parts of the coast have benefitted from massive recovery between 2014 and 2017. However, locally, profiles have continued to retreat during the winters of 2014-2017. Dune fronts have not significantly prograded since the massive erosion of winter 2013-2014.

The coast of Landes shows a noticeable rhythm of progradation at the upper beach/foredune, dune foot and dune front proxies, benefiting from a smaller impact during the 2013-2014 winter and abundant sand being available. Beaches of this part of the coast appear to be stable or in accretion, leading to dune front progradation in some locations since 2011.

Three and a half years after the 2013-2014 winter, the sediment budgets at a regional scale suggest that the major part (86.5 %) of the sand taken from the beach by cross-shore processes have moved back to the beach-dune interface. However, massive sand volume has returned, moving southward following the dominant longshore drift and accentuating the sediment deficit in the northern cell of the coast (Cell 1, 2, 3.1 and 3.2). Many questions remain concerning the cross-shore and the longshore migration of the sand during the winter of 2013-2014 and during the observed recovery sequence in 2014-2017. This analysis was based only on topographic data and must be further investigated and supported by complementary studies dedicated to analyzing the behavior of the subtidal beaches during this period.

Pluridecal trends of coastal evolution are consistent with LiDAR and d-GPS analyses covering the recent period. Comparison with ortho-photography from 1985 suggests no significant acceleration of the erosion rate along the coast during last decade even when the effects of the 2013-2014 winter are considered.

Taking into account that dune front recovery (shape and position) can take decades with an adequate sediment supply, the progressive recovery tendency observable at the beach-dune interface is fragile, particularly in the case of central and south Gironde, where sediments are mainly stocked between the upper beach and the dune foot and are potentially removable by storm marine processes. Even if the sediment budget from the upper beach to the dune is negative between 2011 and 2017 (~ 2 000 × 10^3 m^3) along the 230 km of the Aquitiaine coast, the coastal system of the Aquitaine coast still has a high possibility of recovering in a few years. The massive sediment loss observed after the great winter of 2013-2014 at the beach-dune interface was recovered in most parts of the coast. After several years of relatively moderately energetic conditions and favorable winds, the upper beach has been recolonized, constituting foredunes and even generating dune front progradation. These results illustrate the relevance of the policies in place in the Aquitaine coast, based on soft sediment management and preventing coastline fixation and massive structures as much as possible along the coast. Sustainable sediment management must be organized at a regional scale by taking into account potential interannual massive cross-shore and alongshore dynamics.

Acknowledgments:

The authors are grateful to the Observatoire de la Côte Aquitaine (OCA) for providing data resources in partnership with the ONF and the IGN for LiDAR Data. All cofunders of the OCA project are thanked, namely, the European Union via the FEDER fund, the SGAR, the Région Nouvelle-Aquitaine, and the department of Gironde, Landes and Pyrénées-Atlantiques. The authors want to gratefully acknowledge the anonymous reviewers for their constructive criticism and insightful comments that greatly improved the manuscript.

Bibliography :

Aleman, N., Robin, N., Certain, R., Anthony, E. J., & Barusseau, J. P. (2015). Longshore variability of beach states and bar types in a microtidal, storm-influenced, low-energy environment. Geomorphology, 241, 175-191.

Almeida L.P. , Vousdoukas M.V. , Ferreira Ó. , Rodrigues B.A, Matias A. (2012), Thresholds for storm impacts on an exposed sandy coastal area in southern Portugal Geomorphology, 143–144 pp. 3-12, 10.1016/j.geomorph.2011.04.047

Andrews, B., Gares, P.A., Colby, J.D., (2002). Techniques for GIS modeling of coastal dunes. Geomorphology, 48(1-3), 269-287.

Angnuureng, D. B., Almar, R., Senechal, N., Castelle, B., Addo, K. A., Marieu, V., & Ranasinghe, R. (2017). Shoreline resilience to individual storms and storm clusters on a meso-macrotidal barred beach. Geomorphology, 290, 265-276.

Aubie, S. and Tastet, J.-P., 2000. Coastal erosion, processes and rates: an historical study of the Gironde coastline, southwestern France. Journal of Coastal Research, 16(3), 756-767. West Palm Beach (Florida), ISSN 0749-0208.

Bellesort, B. and Migniot, C., 1987. Catalogue sédimentologie des cotes Françaises. Partie C: de la Gironde à la frontière espagnole, Rapport LCHF-STC, Collection de la Direction des Etudes et Recherches d'Electricité de France, Eyrolles (ed.), pp. 371-552.

Bender, C. J., & Dean, R. G. (2003). Wave field modification by bathymetric anomalies and resulting shoreline changes: a review with recent results. Coastal Engineering, 49(1-2), 125-153.

Bernon N., Mallet C., Belon, R., avec la collaboration de Hoareau A., Bulteau T. et Garnier C. (2016) - Caractérisation de l'aléa recul du trait de côte sur le littoral de la côte aquitaine aux horizons 2025 et 2050. Rapport final. BRGM/RP-66277-FR, 99 p., 48 Ill., 16 tab., 2 ann., 1 CD.

Biausque M And Senechal N. (2018). Storms impacts on a sandy beach including seasonal recovery: alongshore variability and management influences. Revue Paralia, Vol. 11, pp n02.1–n02.16. DOI: https://doi.org/10.5150/revue-paralia.2018.n02

Boak, E. H., & Turner, I. L. (2005). Shoreline definition and detection: a review. Journal of coastal research, 688-703.

Brenner, O. T., Lentz, E. E., Hapke, C. J., Henderson, R. E., Wilson, K. E., & Nelson, T. R. (2018). Characterizing storm response and recovery using the beach change envelope: Fire Island, New York. Geomorphology, 300, 189-202.

Brock, J. C., & Purkis, S. J. (2009). The emerging role of lidar remote sensing in coastal research and resource management. Journal of Coastal Research, 1-5.

Bulteau T., Mugica J., Mallet C., Garnier C., Rosebery D. Maugard F., Nicolae Lerma A., Nahon A. and Millescamps B. (2014). Evaluation de l'impact des tempêtes de l'hiver 2013-2014 sur la morphologie de la côte Aquitaine. Rapport final BRGM/RP-63797-FR, 68p.

Bulteau T., Nicolae Lerma A., and Mugica J. (2016). Caractérisation de l'exposition du littoral Aquitain à l'aléa submersion marine. Rapport final. BRGM/RP-63802-FR

Bulteau, T., Paris, F., Nicolae Lerma, A., Muller, H. (2019) - Le réseau tempêtes de l'Observatoire de la Côte Aquitaine. Rapport final. BRGM/RP-67418-FR, 72 p

Burvingt, O., Masselink, G., Russell, P., & Scott, T. (2017). Classification of beach response to extreme storms. Geomorphology, 295, 722-737.

Castelle, B., Bonneton P., Dupuis H., Sénéchal N. (2007). Double bar beach dynamics on the high-energy meso-macrotidal French Aquitanian coast, Marine Geology, 254 216-223.

Castelle, B., Marieu, V., Bujan, S., Splinter, K. D., Robinet, A., Sénéchal, N., & Ferreira, S. (2015). Impact of the winter 2013–2014 series of severe Western Europe storms on a double-barred sandy coast: Beach and dune erosion and megacusp embayments. Geomorphology, 238, 135-148.

Castelle, B., Bujan, S., Ferreira, S., & Dodet, G. (2017). Foredune morphological changes and beach recovery from the extreme 2013/2014 winter at a high-energy sandy coast. Marine Geology, 385, 41-55.

Castelle, B., Guillot, B., Marieu, V., Chaumillon, E., Hanquiez, V., Bujan, S., & Poppeschi, C. (2018). Spatial and temporal patterns of shoreline change of a 280-km high-energy disrupted sandy coast from 1950 to 2014: SW France. Estuarine, Coastal and Shelf Science, 200, 212-223.

Coco, G., Senechal, N., Rejas, A., Bryan, K. R., Capo, S., Parisot, J. P., J.A.Brown, MacMahan, J. H. (2014). Beach response to a sequence of extreme storms. Geomorphology, 204, 493-501.

De Winter, R. C., Gongriep, F., & Ruessink, B. G. (2015). Observations and modeling of alongshore variability in dune erosion at Egmond aan Zee, the Netherlands. Coastal Engineering, 99, 167-175.

Dissanayake, P., Brown, J., and Karunarathna, H., 2015. Impacts of storm chronology on the morphological changes of the Formby beach and dune system, UK, Nat. Hazards Earth Syst. Sci., 15, 1533-1543, https://doi.org/10.5194/nhess-15-1533-2015, 2015.

Doyle, T. B., & Woodroffe, C. D. (2018). The application of LiDAR to investigate foredune morphology and vegetation. Geomorphology, 303, 106-121.

Esteves, L.S., Brown, J., Williams, J.J., Lymbery, G. (2012). Quantifying thresholds for significant dune erosion along the Sefton coast, Northwest England. Geomorphology 143144, 52–61.

Gonçalves, J. A., & Henriques, R. (2015). UAV photogrammetry for topographic monitoring of coastal areas. ISPRS Journal of Photogrammetry and Remote Sensing, 104, 101-111.

Hesp, P. (2002). Foredunes and blowouts: initiation, geomorphology and dynamics. Geomorphology, 48(1-3), 245-268.

Houser, C., Hapke, C., & Hamilton, S. (2008). Controls on coastal dune morphology, shoreline erosion and barrier island response to extreme storms. Geomorphology, 100(3-4), 223-240.

Houser, C., & Hamilton, S. (2009). Sensitivity of post-hurricane beach and dune recovery to event frequency. Earth Surface Processes and Landforms, 34(5), 613-628.

Houser, C. (2013). Alongshore variation in beach–dune morphology: implications for barrier island response. Geomorphology 199, 48–61.

Houser, C., Wernette, P., Rentschlar, E., Jones, H., Hammond, B., & Trimble, S. (2015). Post-storm beach and dune recovery: Implications for barrier island resilience. Geomorphology, 234, 54-63.

Idier, D., Castelle, B., Charles, E., & Mallet, C. (2013). Longshore sediment flux hindcast: spatio-temporal variability along the SW Atlantic coast of France. Journal of Coastal Research, 65(sp2), 1785-1790.

Irish, J. L., & White, T. E. (1998). Coastal engineering applications of high-resolution lidar bathymetry. Coastal Engineering, 35(1-2), 47-71.

Keijsers JGS, Poortinga A, Riksen MJPM, Maroulis J (2014) Spatio-Temporal Variability in Accretion and Erosion of Coastal Foredunes in the Netherlands: Regional Climate and Local Topography. PLoS ONE 9(3)

Keijsers, J. G. S., De Groot, A. V., & Riksen, M. J. P. M. (2015). Vegetation and sedimentation on coastal foredunes. Geomorphology, 228, 723-734.

Komar, P.D. (1971). Nearshore cell circulation of the formation of giant cusps. Geol. Soc. Amer. Bull. 82, 2643-2650.

Le Mauff, B., Juigner, M., Ba, A., Robin, M., Launeau, P., & Fattal, P. (2018). Coastal monitoring solutions of the geomorphological response of beach-dune systems using multi-temporal LiDAR datasets (Vendée coast, France). Geomorphology, 304, 121-140.

Le Nindre Y.M., Benhammouda S., Rouzeau O., Haas H., Quessette J.A. (2001) - Elaboration d'un outil de gestion prévisionnelle de la côte Aquitaine. Phase 3 : diagnostic d'évolution et recommandations. Contribution du BRGM, BRGM/P-0822-FR, 115p., 55 fig., 5 tabl., 2 ann.

Masselink, G., Castelle, B., Scott, T., Dodet, G., Suanez, S., Jackson, D., & Floc'h, F. (2016). Extreme wave activity during 2013/2014 winter and morphological impacts along the Atlantic coast of Europe. Geophysical Research Letters, 43(5), 2135-2143.

Matias, A., Ferreira, Ó., Dias, J. A., & Vila-Concejo, A. (2004). Development of indices for the evaluation of dune recovery techniques. Coastal Engineering, 51(3), 261-276.

Nicolae Lerma, A., Bulteau, T., Lecacheux, S., & Idier, D. (2015). Spatial variability of extreme wave height along the Atlantic and channel French coast. Ocean Engineering, 97, 175-185.

Nicolae Lerma, A., Bulteau, T., Muller, H., Decarsin, C., Gillet, R., Paris, F., Biausque M., Senechal,N. & Castelle, B. (2018). Towards the Development of a Storm Erosion EWS for the French Aquitaine Coast. Journal of Coastal Research, 85(sp1), 666-670.

Ollerhead, J., Davidson-Arnott, R., Walker, I. J., & Mathew, S. (2013). Annual to decadal morphodynamics of the foredune system at Greenwich Dunes, Prince Edward Island, Canada. Earth Surface Processes and Landforms, 38(3), 284-298.

Orzech, M. D., Reniers, A. J. H. M., Thornton, E. B. & MacMahan, J. H. (2011). Megacusps on rip channel bathymetry: Observations and modeling. Coastal Engineering, 58, 890-907.

Pastol, Y. (2011). Use of airborne LIDAR bathymetry for coastal hydrographic surveying: the French experience. Journal of Coastal Research, 6-18.

Pedreros, R. (2000). Quantification et modélisation du transport éolien au niveau des zones côtières: application au littoral girondin (Doctoral dissertation, Bordeaux 1).

Phillips, M. S., Harley, M. D., Turner, I. L., Splinter, K. D., & Cox, R. J. (2017). Shoreline recovery on wave-dominated sandy coastlines: the role of sandbar morphodynamics and nearshore wave parameters. Marine Geology, 385, 146-159.

Pye, K., & Blott, S. J. (2016). Assessment of beach and dune erosion and accretion using LiDAR: impact of the stormy 2013–14 winter and longer term trends on the Sefton Coast, UK. Geomorphology, 266, 146-167.

Pye, K., Neal, A. (1994). Coastal dune erosion at Formby Point, north Merseyside, England: causes and mechanisms. Mar. Geol. 119, 39–56.

Richter, A., Faust, D., & Maas, H. G. (2013). Dune cliff erosion and beach width change at the northern and southern spits of Sylt detected with multi-temporal Lidar. Catena, 103, 103-111.

Sallenger Jr, A. H., Krabill, W. B., R. N. Swift, J. Brock, J. List, Mark Hansen,. Holman R. A, Manizade S., Sontag J., Meredith A., Morgan K., Yunkel J. K., Frederick E. B. and Stockdon H. (2003). Evaluation of airborne topographic lidar for quantifying beach changes. Journal of Coastal Research, 125-133.

Sallenger, A.H., 2000. Storm impact scale for barrier islands. J. Coast. Res. 16, 890–895.

Saye, S. E., Van der Wal, D., Pye, K., & Blott, S. J. (2005). Beach–dune morphological relationships and erosion/accretion: an investigation at five sites in England and Wales using LIDAR data. Geomorphology, 72(1-4), 128-155.

Schupp, C. A., McNinch, J. E., & List, J. H. (2006). Nearshore shore-oblique bars, gravel outcrops, and their correlation to shoreline change. Marine Geology, 233(1-4), 63-79.

Scott, T., Masselink, G., O'Hare, T., Saulter, A., Poate, T., Russell, P., M. Davidson, Conley, D. (2016). The extreme 2013/2014 winter storms: Beach recovery along the southwest coast of England. Marine Geology, 382, 224-241.

Senechal, N., Coco, G., Castelle, B., & Marieu, V. (2015). Storm impact on the seasonal shoreline dynamics of a meso-to macrotidal open sandy beach (Biscarrosse, France). Geomorphology, 228, 448-461.

Splinter, K.D., Carley, A., Golshani, A., Tomlinson, R. (2014). A relationship to describe cumulative impact of storm clusters on beach erosion. Coast. Eng. 83, 49–55.

Stockdon, H. F., Holman, R. A., Howd, P. A., & Sallenger Jr, A. H. (2006). Empirical parameterization of setup, swash, and runup. Coastal engineering, 53(7), 573-588.

Thornton, E. B., MacMahan, J., & Sallenger Jr, A. H. (2007). Rip currents, mega-cusps, and eroding dunes. Marine geology, 240(1-4), 151-167.

Tucker, M.J. and Pitt, E.G. (2001). Waves in ocean engineering, In Bhattacharyya, R.; McCormick, M.E. (1st ed.). Oxford: Elsevier. pp. 35–36.

Turner, I. L., Harley, M. D., & Drummond, C. D. (2016). UAVs for coastal surveying. Coastal Engineering, 114, 19-24.

Vellinga, P. (1982). Beach and dune erosion during storm surges. Coast. Eng. 6, 361–367.

Vousdoukas, M. I., Almeida, L. P. M., & Ferreira, Ó. (2012). Beach erosion and recovery during consecutive storms at a steep-sloping, meso-tidal beach. Earth Surface Processes and Landforms, 37(6), 583-593.

Wang, P., Kirby, J. H., Haber, J. D., Horwitz, M. H., Knorr, P. O., & Krock, J. R. (2006). Morphological and sedimentological impacts of Hurricane Ivan and immediate poststorm beach recovery along the northwestern Florida barrier-island coasts. Journal of Coastal Research, 1382-1402.

Woolard, J. W., & Colby, J. D. (2002). Spatial characterization, resolution, and volumetric change of coastal dunes using airborne LIDAR: Cape Hatteras, North Carolina. Geomorphology, 48(1-3), 269-287.

Tables:

Table 1: Nearshore system and beach-dune main characteristics along the Aquitaine coast

Cell	Nearshore bar system	Outer bar shape	Outer bar length	Inner shape	Inner bar (bar rip channel) length	Berm	Beach width	Beach/dune contact	granulometry	Dune height	Dune evolution scenario / or / System evolution
Cell 1	unpronounced	-	-	-	Temporal	No / small (~0.5m)	20 m	Dune scarp and paleosoil	Sand	10 to 15 m	Natural and fixed (protection). Strong erosion (>2m/y)
Cell 2	uniform longshore bars	straight	-	Straight with unpronounced transverse rip channel	-	No / small (~0.5m)	20 to 40 m)	Dune scarp and paleosoil	Gravel / sand	15 to 20 m	Low erosion (~1m/y)
Cell 3	Double bars	Crescentic and tridimensional	600 - 1 000 m	Almost periodic, deep transverse rip channel	200 to 400 m	North : not established (~0.5m) or small (~0.5m) ? South : Crescentic	100 to 200 m	Rare to frequent established foredune	sand	12 to 25 m	North: strong erosion (>2m/y) South: low erosion (1m/y)
Cell 4	variable	-	-	-	-	Variable	Highly variable	Beach scarp to established foredune	Sand	15 to 25 m	Tidal delta dynamics / sandspit : variable evolution potentially strong erosion (>2m/y)
Cell 5	Double or triple bars	Cresentic and tridimensional	800 - 1200 m	Periodic, deep transverse rip channel	200 to 500 m	Crescentic	200-300 m	Frequent established foredune	Sand	15 to 25 m	Low erosion or stable (<2m/y)
Cell 6	Double bars	cresentic	Irregular, 400-1000 m	Almost perpendicular rip channel	Irregular	Crescentic, frequently doubled	100-120 m	Beach scarp to established foredune	Sand / Coarse sand	15 to 20 m	North: high erosion (>2m/y) South: low erosion (1m/y), locally stable
Cell 7	Double bars	straight	-	Straight with perpendicular rip channel		No / small (~0.5m)	150 to 200 m	Artificialized	Gravel / sand	10 to 15 m	Beach stable, subtidal beach in erosion

Table 2: LiDAR campaigns

Campaign	**Date of the survey**	**Altimetric estimated error Z (m)**
LiDAR 2011	5 March to 21 May 2011	0.196
LiDAR 2014	23 - 24 October 2014	0.144
LiDAR 2016	29 - 30 October 2016	0.106
LiDAR 2017	4 - 6 and 7 October 2017	0.102

Table 3: Rates of coastline evolution along the Aquitaine coast at pluri-annual, decadal and pluri-decadal time scales, in m/year

Data	Cell 1	Cell 2	Cell 3	Cell 4	Cell 5	Cell 6
LiDAR (2011-2017)	-4.2	-1.4	-0.7	-1.0	-0.1	-1.7
D-GPS (2006-2017)	-5.3	-4.5	-1.0	-2.5	-0.4	-3.5
Orthophotography (1985-2014) Mean trend	-2.5	-1.1	-0.9	-2.5	-0.5	-1.7
Orthophotography (1985-2014) Mean trend - std	-0.5	-0.9	-0.4	-0.8	-0.3	-0.9
Orthophotography (1985-2014) Mean trend + std	-4.5	-1.3	-1.4	-4.1	-0.8	-2.6